Emissions from a Domestic Wood Heating Appliance: Experimental Measurements and Numerical Study Using an Equivalent Reactor Network (ERN) Approach Coupled with a Detailed Chemical Mechanism

Joseph Darido, Amal Dhahak, Roda Bounaceur, Céline Le Dreff - Lorimier, Gontrand Leyssens, Fabrice Cazier, Paul Genevray, Frédérique Battin-Leclerc

Emissions from a domestic wood heating appliance: experimental measurements and numerical study using an equivalent reactor network (ERN) approach coupled with a detailed chemical mechanism

Joseph Darido[a,#], Amal Dhahak[a,#], Roda Bounaceur[a], Céline Le Dreff - Lorimier[b], Gontrand Leyssens[c], Fabrice Cazier[d], Paul Genevray[d], Frédérique Battin-Leclerc[a,]*

[a] Université de Lorraine, CNRS, LRGP (Laboratoire Réactions et Génie des Procédés), F-54000 Nancy, France

[b] Centre Scientifique et Technique du Bâtiment (CSTB), F-44323 Nantes, France

[c] Université de Haute-Alsace, LGRE (Laboratoire Gestion des Risques et Environnement), F-68093 Mulhouse, France

[d] Université du Littoral Côte d'Opale, CCM (Centre Commun de Mesures), F-59140 Dunkerque, France

* Corresponding author: frederique.battin-leclerc@univ-lorraine.fr

[#] These authors contributed equally to this work.

ABSTRACT

Dwindling fossil fuel reserves and global climate change drive researchers to discover and develop new strategies to derive energy from renewable sources, such as biomass, including wood. However, when poorly controlled, wood burning can be a source of atmospheric pollution. With the ultimate purpose of better controlling pollutant emissions from domestic small combustion installations, this paper follows two objectives. Firstly, temperature and pollutant measurements obtained at the chimney outlet of a domestic inset fed with wood logs and working under nominal operating conditions are presented. Measured pollutants include CO, CO_2, nitrogen oxides (NOx), mono-aromatic, carbonyl and phenolic compounds, as well as polycyclic-aromatic hydrocarbons (PAHs) and sugars with measurement made using different types of wood. Secondly, this paper describes a first attempt of modeling based on a detailed chemistry and test it for simulating the measured pollutants. The model includes a previously developed detailed chemical kinetic mechanism and a simplified model of thermal transfer in the wood log. A network of ideal reactors (equivalent reactor network (ERN)), for which simulations using the detailed kinetic model are feasible, is proposed to represent both the primary pyrolysis and the combustion of the emitted gaseous species. With only adjusting the parameters used in the model in order to well simulate the smoke temperature and the CO_2 mole fraction for a single batch, simulations give a reasonably good order of magnitude for all the measured pollutants for the seven used wood batches. A sensitivity analysis of the used parameters and of the structure of the ERN model is also presented.

Keywords: Combustion; biomass; pollutant emission; detailed kinetic model; heat transfer; Equivalent Reactor Network (ERN).

TOC Graphic

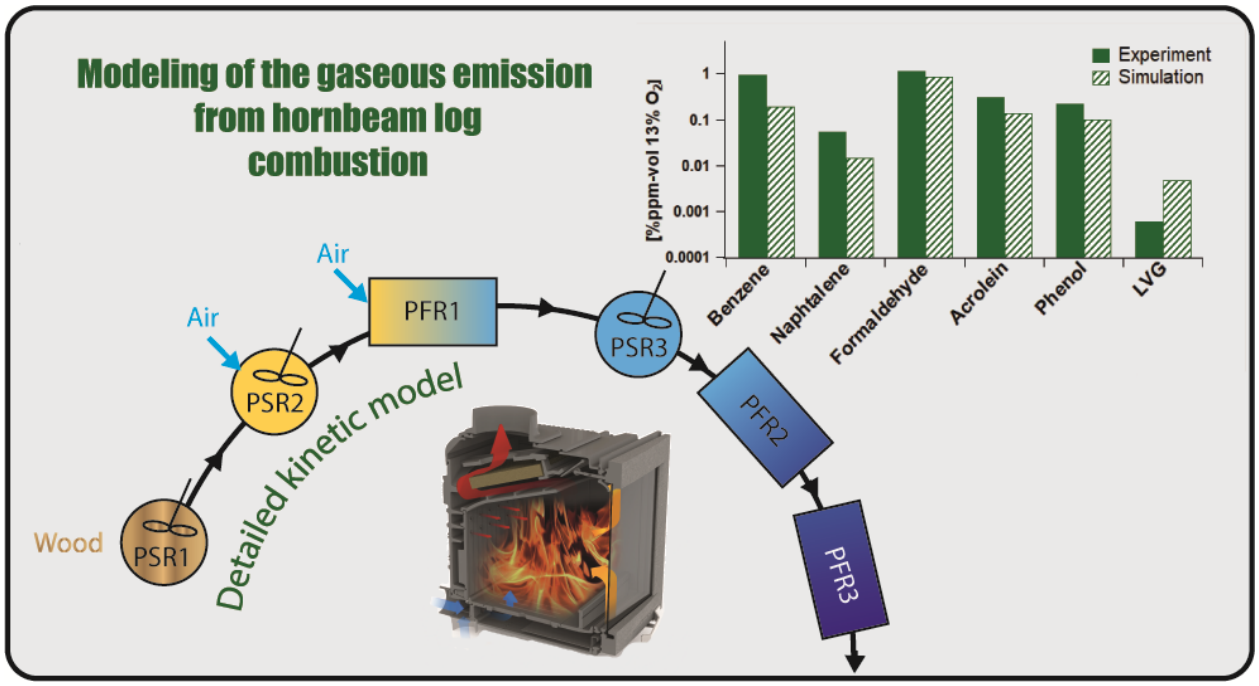
Modeling of the gaseous emission from hornbeam log combustion
Air
Air
PFR1
PSR2
PSR3
PFR2
PFR3
PSR1
Wood
Detailed kinetic model
[%ppm-vol 13% O2]
1
0.1
0.01
0.001
0.0001
Experiment
Simulation
Benzene
Naphtalene
Formaldehyde
Acrolein
Phenol
LVG

Symbols and Abbreviations

Symbols	
Cp	specific heat
e	thickness
H	height
L	width
m	mass
M	mass flow rate
n	moles number
Q	heat quantity
t	time
T	temperature
x, y	spatial variables
α	absorption coefficient
α_{stoich}	stoichiometry coefficient
ε	surface emission factor
σ	Stephan constant
λ_t	thermal conductivity
ρ	density
τ	residence time
ϕ	equivalence ratio

Abbreviations	
BTEX	Benzene, Toluene, Ethylbenzene, Xylenes
CCM	**Centre Commun de Mesures**
CFD	Computational Fluid Dynamics
CSTB	**Centre Scientifique et Technique du Bâtiment**
ERN	Equivalent Reactor Network
Exp	Experiments
FEM	Finite element Method
HAA	hydroxyacteldehyde
HC	hydrocarbons
HMFU	hydroxymethlfurfural
LGRE	**Laboratoire Gestion des Risques et Environnement**
LVG	Levoglucosan
PAH	polycyclic aromatic hydrocarbons
PaSPFR	Partially Stirred Plug Flow Reactor
PaSR	Partially Stirred Reactor
PFR	Plug flow reactor
PSR	Perfectly Stirred Reactor
Sim	Simulations
SM	Supplementary Materials
Stoich	Stoichiometry
TVOC	Total Volatile Organic Compounds
US-EPA	United States Environmental Protection Agency

Introduction

Wood is an important local source of energy in many countries. In European countries, wood contributes to 45% of the primary energy mix from renewable sources[1]. In addition, wood manufacture produces a variety of products, which assure the forest-based sector growth and provide many job opportunities. Being renewable, reusable and recyclable, wood is today a globalized commodity.

With the current global warming issues because of the increasing emission of CO_2[2], renewable resources and especially biomass, is set to become, at least for the near future, an important solution to the energy need and the environmental issues. Wood is a carbon-neutral renewable source of energy, provided that the forests from which the wood is grown, are managed in a sustainable manner[3,4].

Wood, the first renewable energy in France and Europe, is mainly used for domestic combustion installations[5]. However, crucial problems can be associated with such a fuel. Biomass combustion may emit different types of pollutants, such as fine particles and gaseous pollutants (carbon, sulfur and nitrogen oxides, oxygenated hydrocarbons (HC), polycyclic aromatic hydrocarbons (PAH)…)[6,7,8]. In order to understand, control and reduce pollutant emissions from wood-burning appliances, a complete description of the combustion is needed including the chemical mechanisms of formation of these pollutants and the involved parameters.

Biomass combustion and gasification are very complex processes, since they include three aspects: chemical kinetics, mass and heat transfer and aeraulics. As described by Andersson et al.[9], three approaches were previously used in the literature to model biomass combustion and gasification: single biomass particles combustion models, models of a full combustion device based on Computational Fluid Dynamics (CFD) and models using a multiscale Equivalent Reactor Network (ERN).

Single fuel particle modeling is an efficient approach to investigate intra-particle heat and mass transfer during biomass thermal degradation. Lu et al.[10] used a single-particle reactor to study the combustion of poplar particles with different shapes (flat plate, sphere and cylinder). A two-stage kinetic model described the devolatilization of wood in light gas, tar and char and the gas-phase combustion scheme included three global reactions of volatiles species (CO, CO_2 and hydrocarbons represented by the lumped molecule $C_6H_{6.2}O_{0.2}$). Heat, mass and momentum transfer equations were established for both solid and gas phases. The developed model was used to simulate the resulting flame around the particle surface during combustion. Single particle combustion was experimentally and numerically investigated by Yang et al.[11] using cylindrical particles. Transport equations were written for gas phase, solid phase and moisture. Biomass devolatilization was represented by one global reaction decomposing solid into char and volatiles represented by the lumped molecule $C_mH_nO_l$. While it can be based on a detailed model of the thermal transfer inside the particle, the single particle approach using global reactions cannot be an appropriate method to model pollutant formation during biomass combustion in insets, stoves and industrial systems because of its simplified chemistry.

CFD is the most used approach to model combustion appliances because of the complexity of the problem and the interaction between several disciplines[12]. In general, CFD models are coupled to simplified kinetic mechanisms. Porterio et al.[13] developed a CFD model to study biomass combustion in a pellet domestic boiler. They used three global reactions to model dry wood devolatilization in gas, tar and char, a global reaction to describe char oxidation, and five global reactions to describe the gas-phase oxidation of volatiles compounds, considered as a mixture of CO, CO_2, H_2, CH_4 and C_6H_6. Tabet et al.[14] modelled combustion in domestic biomass heating appliances to estimate CO and CO_2 emissions. Biomass degradation was described by a fluidized bed model, in which a wood log was subdivided in three layers, where wood drying, wood pyrolysis and char burning occurred, respectively. Two competitive global

reactions were used to model biomass devolatilization into light volatiles, heavy volatiles and two residues, which were then oxidized by a few global reactions. The global CFD stove model was obtained by coupling the bed model and the gas-phase model representing hydrocarbons combustion (three global reactions). A one-step global reaction was used by Kausley and Pandit[15] to model biomass pyrolysis in their study concerning solid fuel combustion in domestic stoves. Furthermore, volatiles combustion was modeled by three global reactions. CFD approach has been proven to be a valuable tool to model aeraulics, mass and heat transfer in a combustion appliance but it is limited in terms of pollutants predictions. This is because, as shown by the previous examples, this approach still implies the use of very small kinetic models unable of representing the complex chemistry involved in the combustion of biomass, and therefore cannot be used to follow the formation of pollutants.

The ERN approach can be a way to model a combustion appliance using a more complete chemistry. This approach is mainly used to model the thermal degradation and gasification of biomass. It also allows modelling the aeraulics in complex systems in a simplified way, with the advantage of using detailed kinetic models. ERN model can be coupled to CFD approach to optimize industrial systems[16]. Andersson et al.[9] developed an ERN model, based on ideal reactor (Perfectly Stirred Reactor (PSR) and Plug Flow Reactor (PFR)) to reproduce an entrained flow biomass gasifier in order to optimize operational parameters. The pyrolysis was represented by a one-step reaction while nine global reactions were used to describe the gas-phase reactions. To represent thermal degradation of biomass in a drop tube reactor, Weber et al.[17] developed an ERN composed of Partially Stirred Reactors (PaSR) coupled to a Partially Stirred Plug Flow Reactor (PaSPFR). Using a generic formula of wood ($C_{42}H_{64}O_{28}$), their kinetic model consisted of a global devolatilization reaction coupled to five secondary gas phase reactions and three oxidation reactions of the produced char. Menage et al.[18] developed an ERN composed of PSR reactors to study the high heating rate devolatilization and oxidation

of coals in a flat flame reactor under several conditions. To predict O_2, CO_2, CO, NO and SO_2 concentration profiles, they used a global devolatilization reaction coupled to a detailed kinetic model for gas-phase combustion (868 reactions) and four char oxidation reactions. An ERN was also constructed by Stark et al.[19] to model the gasification of woody biomass in a fluidized bed reactor, in order to predict the formation and the evolution of tar and gas species. The ERN considered a PSR to reproduce the fluidized bed region and a PFR for the freeboard. They used a semi-detailed mechanism from the literature[20] to represent solid devolatilization and gas-phase reactions, performing kinetic modeling using the software CHEMKIN-PRO®. Das et al.[22] modeled a bubbling fluidized bed biomass gasifier using also an ERN. They optimized and used a version of the detailed chemical kinetic model "CRECK", coupled with their ERN that contained 3 zones. The pyrolysis zone modeled using a thermodynamic equilibrium model placed in succession with a PSR. The gasification zone and the freeboard zone were simulated by a PSR and a PFR respectively.

The main aim of this paper is to develop and test a new model of combustion in a wood inset in order to simulate polluting emissions. In line with the idea of Menage et al.[18], Stark et al.[19], Das et al.[22], the wood heating appliance is modeled by the ERN approach, using a detailed kinetic model. The kinetic mechanism is based on a previous one tested against a wide range of experimental results published in the literature, as described in a previous work[23]. The ERN model coupled with the kinetic mechanism and a simplified thermal model has been tested for predicting new measurements for a wide range of pollutants at the outlet of a domestic inset fed with wood logs.

I. Experimental approach and results

The experiments were performed in LGRE (Laboratoire Gestion des Risques et Environnement) in Mulhouse in collaboration with CCM (Centre Commun de Mesures) and CSTB (Centre Scientifique et Technique du Bâtiment). The set-up consists of a wood inset connected to an instrumented chimney equipped with thermocouples and gas analyzers. The objective of these measurements was to gather data from the emission of combustion performed on several samples of wood. The set-up will be described in this paragraph, followed by a detailed list of the collected data.

I.1. Description of the wood inset and of its outlet

Combustion tests were performed in a wood inset (named XP68-IN and commercialized by LORFLAM) as is shown on Fig.1.a. This wood inset model has the following dimensions (height x width x depth) 60 cm x 68 cm x 54 cm as schematized in Fig.1.b. along with the experimental set up dimensions (not to scale).

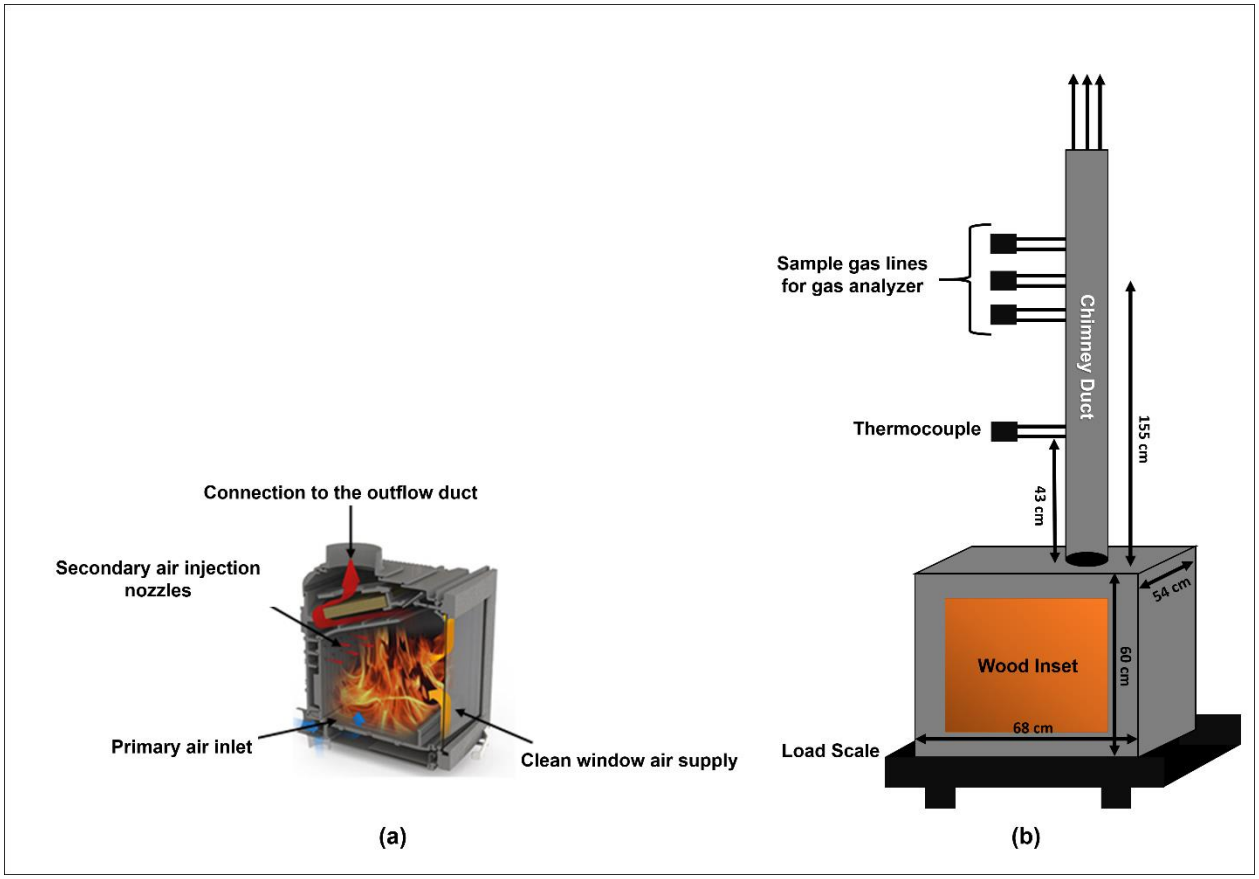

Fig.1. Experimental device: (a) XP68-IN wood inset; (b) Scheme of the set-up used for the experimental combustion tests with dimensions (not to scale).

In order to characterize the combustion gas composition, sample lines for gas analysis were located at an average distance of 155 cm in the chimney duct, to measure the emissions during the experiments on the inset. The highest line was used for PAHs and the lowest one for CO, CO_2, NO; both lines were about 71 cm apart. The smoke temperature was measured via a thermocouple placed 43 cm from the inset. According to NF EN 13229 standard, concentrations expressed in $mg.Nm^{-3}$ were referred to 13% of O_2 in the exhaust to insure comparison for all experiments. Main gaseous compounds (O_2, CO, CO_2, SO_X and NO) were analyzed by specific analyzers Hartmann & Braun–Magnos 6G and URAS 10P. Total Volatile Organic Compounds (TVOC) and TVOC without methane were recorded by a flame ionization detector Cosma Graphite 655 and were expressed in equivalent CH_4. In addition, a sampling

device (CATECO model) provided by CleanAir EUROPE allowed sampling in isokinetic conditions. This device consists of a heated sampling probe connected to a heated filter holder, maintained at a temperature of 120 °C, followed by a refrigerated collecting system to condense water vapor and collect gaseous volatile organic compounds on a resin trap. The whole system was connected to a sampling pump and a flow control device. For PAH and phenolic compounds analysis, a half of each filter and the XAD-2 resin (Restek – Ultraclean Resin) collected were submitted to a Soxhlet extraction by dichloromethane/acetone (50/50) during 24 hours, and condensates were treated by liquid/liquid extraction with dichloromethane only. For the organic biomass combustion tracers (e.g. levoglucosan, mannosan, galactosan), the other half of the filter was sonicated in ethyl acetate during 1 hour and then derivatized. The extracts obtained were concentrated under nitrogen flux and analyzed by GC/MS (VARIAN 3800/1200 TQ). COV as BTEXT were trapped on TENAX cartridge, and aldehydes/ketones on DNPH cartridge connected to a sampling pump equipped with flow control device. TENAX cartridges were then thermally desorbed with a thermodesorber (Perkin Elmer TurboMatrix TD) equipped with a cold trap, before being analyzed by GC/MS (PerkinElmer Clarus 680). DNPH cartridges were eluted with acetonitrile and then analyzed by HPLC coupled with a Photo Diode Array detector (Waters Alliance 2695/PDA 996).

Seven samples of wood were studied in order to characterize the impact on emissions of the species of wood, its origin and the way it is prepared before burning: five samples of hornbeam wood logs coming from two different batches and prepared either with/without bark and raw/washed, a sample of pine pallets and a sample of commercialized densified wood log. Table 1 gives the physical and chemical properties of the studied woods. Each log of hornbeam had a length of 330 mm and a diameter around 60-80 mm, while densified wood log had a length of 150 mm and a diameter of 90 mm and pieces of pine pallet had a length of 330 mm, a width of 140 mm and a thickness of 24 mm. For all the tests, the standard wood load

introduced consisted of two logs for a total mass of 2.4 kg, which is a common load in modern appliances. The used logs had a very close shape and mass, as the reproducibility of the tests is maximized when the two logs complete their combustion simultaneously.

Table 1: Characteristics of the studied wood samples.

Sample Number		Sample 1	Sample 2	Sample 3	Sample 4	Sample 5	Sample 6	Sample 7
Properties/Wood type		Hornbeam Batch A With Bark	Hornbeam Batch A Without Bark	Hornbeam Batch A With Bark	Hornbeam Batch B With Bark	Hornbeam Batch B Without Bark	Densified log (coniferous)	Pallet (Pine)
		Raw	Raw	Washed	Raw	Raw	Raw	Raw
C (% in dry)[a]		47.7	47.9	47.6	47.1	47.5	47.3	48.9
H (% in dry)[a]		6.1	6.1	6.1	6.0	6.1	6.1	6.2
O (% in dry)[a]		44.6	44.8	44.3	44.3	44.9	44.2	43.5
N (% in dry)[a]		0.2	0.2	0.3	0.2	0.2	0.1	0.3
S (% in dry)[a]		< 0.03	< 0.03	< 0.03	< 0.03	< 0.03	< 0.03	< 0.03
H_2O (% in raw)[a]		12.4	12.3	11.3	11.8	11.8	11.0	26.2
Chemical Composition in Mass fraction[b]								
Mass Fraction	Cellulose	0.4253	0.441	0.4137	0.4508	0.4386	0.4044	0.2973
	Hemicellulose	0.231	0.2395	0.2247	0.2449	0.2383	0.2197	0.1615
	Lignin-H	0.1752	0.168	0.1884	0.1572	0.1643	0.1916	0.2007
	Lignin-O	0.0219	0.0043	0.0381	0.0051	0.0194	0.0543	0.0577
	Lignin-C	0.0226	0.0242	0.022	0.024	0.0213	0.02	0.0209
	H_2O	0.124	0.123	0.113	0.118	0.118	0.11	0.262
Chemical Composition in Mole fraction								
Mole Fraction	Cellulose	0.2224	0.2295	0.2292	0.2387	0.2339	0.2286	0.1003
	Hemicellulose	0.1482	0.153	0.1528	0.1591	0.156	0.1524	0.0669
	Lignin-H	0.034	0.0325	0.0388	0.0309	0.0326	0.0403	0.0252
	Lignin-O	0.0044	0.0009	0.0081	0.001	0.004	0.0118	0.0075
	Lignin-C	0.0074	0.0079	0.0077	0.008	0.0071	0.0071	0.0044
	H_2O	0.5835	0.5762	0.5634	0.5623	0.5664	0.5598	0.7957

[a] Mass fraction of elements measured before the experiments. [b] Calculated from the C, H, O composition by the method of Ranzi et al.[24], and used to get the molar composition of the wood.

For all the tests, the experimental protocol was identical, with:

- An ignition load,
- A warm-up load,
- At least two nominal loads (performed at nominal heat output according to the operating instruction manual of the appliance).

This experimental protocol led to a temperature evolution in the combustion products similar to the one shown in Fig.2.

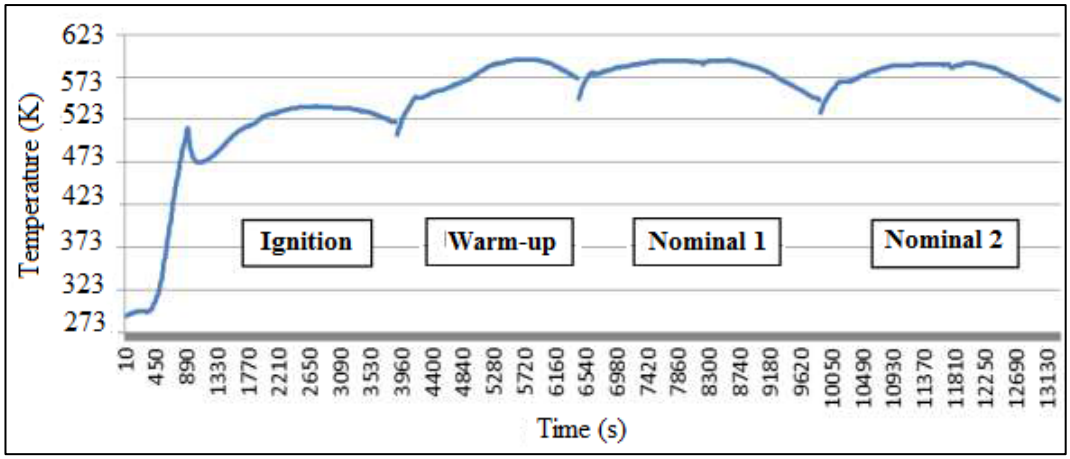

Fig.2. Evolution of flue gas temperature as a function of time.

I.2. Experimental results

The experimental protocol applied in this study is based on EN 13229 and EN 16510-1 standards (with some adjustments) and is similar to the one used in previous studies[7,8]. The experimental results obtained from the combustion of all these samples are shown in two tables provided as Supplementary Material. These tables present the obtained smoke temperatures, as well as the mole fractions in ppm and emission factors in $mg/kg_{dry\ wood}$ (normalized at 13% O_2, for comparison purpose in accordance with NF EN 13229[25]) measured for a selection of different compounds:

- **Common combustion gases** (CO, CO_2, O_2, NO and SO_2),
- **Mono-aromatic compounds** (benzene, toluene, ethylbenzene, xylenes and trimethylbenzene),
- **PAHs** (naphthalene, acenaphthylene, phenanthrene, pyrene, chrysene, *acenaphthene*, *fluorene*, *anthracene*, *fluoranthene*, *benzo[a]anthracene*, *benzo[b]fluoranthene*, *benzo[k]fluoranthene*, *benzo[a]pyrene*, *indeno[1,2,3-c,d]pyrene*, *dibenzo[a,h]anthracene* and *benzo[g,h,i]perylene*),

- **Aldehydes and ketones** (formaldehyde, acetaldehyde, acetone, acrolein, benzaldehyde, *propionaldehyde*, *crotonaldehyde*, *2-butanone*, *methacrolein*, *butyraldehyde*, *valeraldehyde*, m-*tolualdehyde* and *hexaldehyde*),
- **Phenolic compounds** (phenol, guaiacol and syringol),
- **Sugars** (levoglucosan (LVG), *mannosan*, *galactosan*).

The compounds shown in italic, are those for which numerical simulations results are not provided. The selection of the measured chemical species was based on a number of reasons:

- For PAHs: these are the 16 molecules (combustion products) prioritized by the US-EPA (United States Environmental Protection Agency). Note that for these compounds, a reasonable agreement was obtained with the measurements of Tschamber et al.[7].
- For sugars and phenolic compounds: the selected molecules are recognized as being wood combustion tracers.
- For BTEX, aldehydes and ketones: these are volatile organic compounds, characteristic of the combustion phenomena.

II. Modeling of a domestic wood inset through an Equivalent Reactor Network (ERN approach)

The purpose of this modeling work is to use a previously developed detailed kinetic model in order to predict the emission of the here-before listed pollutants at the outlet of a wood inset. Because of the large size of the model, which includes 632 species and 4759 reactions, only simulations using ideal reactors are achievable. This part II then describes the ERN structure which has been considered in order to model the different steps of the combustion process and the different zones in the inset.

II.1. General description of the used ERN approach to be coupled to a detailed chemical model

The processes occurring along the inset from the air inlet until the emissions from the chimney flue have been described using an ERN approach. The network of ideal reactors represents both the primary pyrolysis and the combustion of volatile species.

After several tries, the process of combustion of wood logs inside an inset was divided into steps, each modeled by an ideal reactor as shown in Fig.3. The method used to choose the reactors was impacted by a recent study by Leclerc et al.[21]. The selected reactors are three Perfectly Stirred Reactors (PSR) and three Plug Flow Reactors (PFR), in which a chemical simulation is performed using the software CHEMKIN-PRO®. Two air inlets ("Air 1": for primary combustion and "Air 2": for secondary combustion) are considered. The temperatures at the outlet of each reactor of the developed ERN were obtained by the resolution of the enthalpy balances using this same software.

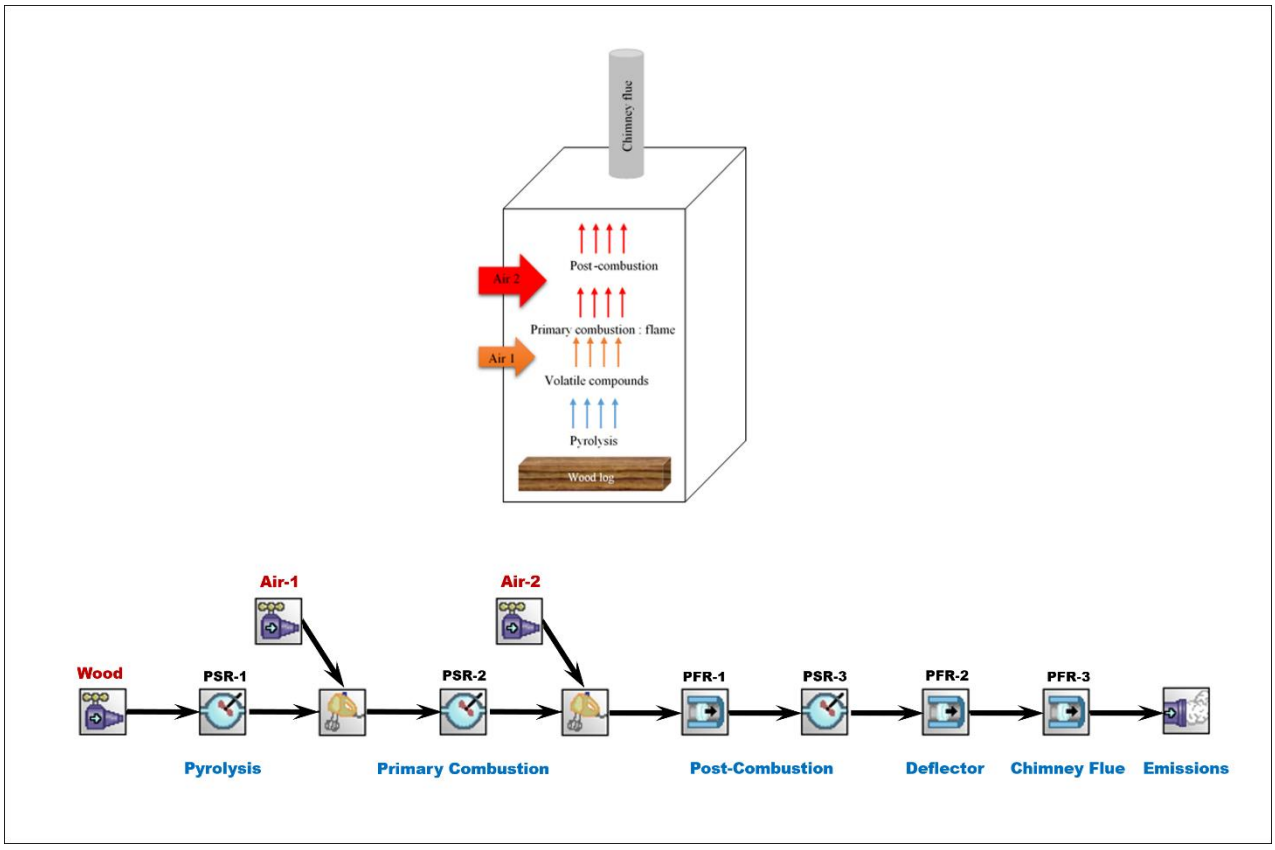

Fig.3. Equivalent Reactor Network constructed in this study: Allocation of the zones in the inset (top) and the corresponding flowsheet in CHEMKIN-PRO® (down).

The chemical model used in this work is an updated version of the BioPOx model described in Dhahak et al.[23]. The modifications are explained in details in part IV. This model includes two parts: a semi-detailed mechanism to describe biomass devolatilization and a detailed mechanism for the produced tar gas-phase combustion. The up-dated version of BioPOx model is available in Supplementary Material.

To predict, control and reduce pollutant emissions from wood appliances for domestic heating, the kinetic model BioPOx had to be coupled to a thermal model. Indeed, for large biomass particles such as wood logs and for high temperatures, physical phenomena such as heat and mass transfer cannot be ignored. This part is explained in chapter III.

II.2. Detailed description of the Equivalent Reactor Network

The six ideal reactors considered in our ERN are described below. As detailed, operating conditions (temperature, inlet composition, residence time …) and reactor design parameters (heat losses, volume...) were either taken from the experimental measurements, estimated from previous work or adjusted to fit the predictions to the experimental measurements of smoke temperature and CO_2 mole fraction during the combustion of a batch of hornbeam logs.

a. Pyrolysis zone: PSR-1

Several studies in the literature have modeled the primary pyrolysis of biomass using a PSR [9,19,26] or a Partially Stirred Reactor (PaSR)[17]. In line with these studies, the first element of the ERN is a PSR that models the pyrolysis of a thin layer of wood on the log surface. The inlet temperature of this reactor (PSR-1) is the average temperature in the considered layer, which is determined after resolution of the thermal balance in the log. The outlet temperature is

obtained after solving the enthalpy balance, considering the endothermicity of the pyrolysis reactions and the thermal losses due to the evaporation of the moisture. The value of these thermal losses, for a whole log, is estimated to 22 cal/s according to the study of Gogoi and Baruah[27] with a wood of 10% moisture content. On the bases of these two values and the surface of each ideal reactor it is possible to get an estimation of the thermal losses of each sub-reactor involved in the ERN.

Assuming that the pyrolysis of the top layer of the log is an almost instantaneous reaction[7,28], the residence time in PSR-1 is considered to vary between 0.001 and 1 s. The PSR-1 feed is composed of wood with a given moisture content. The output of this reactor is a mixture of volatile compounds that will mix with air in the second reactor of the network, PSR-2.

b. Combustion zone: PSR-2

The second element of the network, PSR 2, simulates the oxidation of volatile compounds by oxygen in air. The choice of this type of reactor is based on studies from the literature. Anderson et al.[9] used a PSR to model the flame zone of a gasifier. To predict NOx emissions in gas turbines, Fichet et al.[29] also represented the combustion zones by PSR reactors.

The inlet temperature of PSR-2 is the outlet temperature of PSR-1. The resolution of the enthalpy balance leads to a high increase in the temperature, at the exit of this reactor, around 2000 K. increase. This reactor can be assimilated to the flame zone. In this study, the residence time of the gas mixture in this flame zone is considered to be very short, of the order of 0.005 ms. The primary combustion is assumed to occur in poor mixture and the equivalence ratio in this zone is considered to vary between 0.5 and 1.

Note that this combustion zone is the heart of any device involving wood combustion, but also the trickier to represent using ERN. The proposed attempt is a first extremely simplified approach, which may require further improvements.

c. Post-combustion zone: PFR-1 in series with PSR-3

The post combustion, or double combustion, is modeled thanks to a third perfectly stirred reactor (PSR-3) preceded by a plug flow reactor with an important heat exchange with exterior (PFR-1). The role of this zone is to burn residual volatile compounds exiting PSR-2 by adding preheated secondary air.

After adding the air, the role of PFR-1 is to consider the heat losses in the mixture before it enters the PSR-3, since heat production is the major purpose of a wood stove or inset. However, as it will be seen further in the text, significant chemical changes are also encountered in this zone. The residence time and the heat loss of PFR-1 has been chosen by testing several values in order to get an important decrease of temperature without any overconsumption of CO.

As the post-combustion occurs in a large part of the combustion chamber, the residence time in PSR-3 is considered to vary between 1 to 10 s. This value (10 s) corresponds to the residence time in the empty inset, calculated by dividing the inset volume by the volumetric flow. The secondary combustion is assumed to occur in poor mixture. Therefore, the secondary air inlet is adjusted by fixing the equivalence ratio of PSR-3 below 1. The resulting mixture enters in PFR-2

d. Deflector: PFR-2

The fourth element of the network is a Plug Flow Reactor (PFR-2), which represents the deflector. The deflector ensures the escape of combustion gases from the top of the appliance while maintaining two main roles: preventing the rapid evacuation of gases and increasing the temperature in the combustion chamber. By providing these two functions, the deflector can improve the quality of combustion[30].

As providing by the manufacturer (LORFLAM), the length, width and the thickness of the deflector zone are of 296 mm, 525 mm and 28 mm, respectively. The residence time in PFR-2 is then of the order of 5 ms.

The inlet temperature of PFR-2 is that at the outlet of PSR-3. The outlet temperature of PFR-2 is obtained after resolution of the enthalpy balance, with an adjusted thermal losses of 0.2 cal/(s.cm). The resulting mixture enters PFR-3.

e. Chimney: PFR-3

The last reactor, PFR-3, represents the chimney, in which the emission measurements are performed. This element allows the evacuation of combustion products to the outside. The length and the diameter of the chimney zone are of 155 cm (average value of the position of the different sampling lines) and 15 cm respectively. The residence time in PFR-3 is of the order of 7 s. The inlet temperature of PFR-3 is that at the outlet of PFR-2. The outlet temperature of this reactor (PFR-3) is obtained after resolution of the enthalpy balance considering the heat losses (heat released by the hot gases to the outside). Theses heat losses were adjusted to 1.7 cal/(s.cm), so that the temperature at the outlet of PFR-3 could be compared to the temperature of the combustion products measured experimentally.

The different parameters used for each reactor in the network are summarized in Table 2. These simulations require knowing the temperature on the surface of the log (inlet temperature of PSR-1). For this purpose, a code under the software MATLAB® was developed to solve the heat balance in the log as described in part III. The resolution of this heat balance requires knowing the flame temperature obtained during the combustion of the volatile compounds in PSR-2. An iterative method, by simulating the two zones, pyrolysis (PSR-1) and primary combustion (PSR-2), using the detailed kinetic model BioPOx, allows determining this temperature.

Table 2: The different parameters used for each reactor in the network and their optimization range.

Reactor	Zone	Feed	Tin	Tout	τ (sec)	ϕ [a]
PSR-1	Pyrolysis	Wood	T1	T2	10^{-3} - 1	∞
PSR-2	Oxidation	Volatile species at the exit of PSR-1 + primary air	T2	T3	10^{-5} - 1	< 1
PFR-1	Oxidation heat release	Volatile species at the exit of PSR-2	T3	T4	10^{-5} - 1	< 1
PSR-3	Post-combustion	Volatile species at the exit of PFR-1 + secondary air	T4	T5	1 - 10	no new air inlet
PFR-2	Deflector	PSR3 output	T5	T6	0.005	no new air inlet
PFR-3	Chimney flue	PFR1 output	T6	T7	0.87	no new air inlet

[a] Equivalent Ratio see text below for full description.

III. Development of a simplified thermal model within a wood log

This part will focus on studying, in a simplified way, the heat transfer within a macro-particle, which in this case, is a log of wood. Thanks to the developed thermal model, the profile of the temperature inside the log can be determined.

III.1. Description of the used heat transfer equations

A log with a shape supposed to be parallelepiped with a height H, a width L and a thickness e, is considered. The pyrolysis of biomass is the step that precedes the combustion of the volatile species. During this phase, the wood, which is initially at the inset temperature, decomposes under the effect of heat forming solid residues and releasing gaseous compounds (tars). The combustion of tars by the oxygen of the air is accompanied by the formation of a flame. The heat obtained by the radiation of this flame (Q_{top}) is used to heat the upper layer of the log and to provide the energy necessary to maintain its pyrolysis. The temperature at the surface increases and the heat propagates towards the other layers by conduction, as shown in Fig.4.

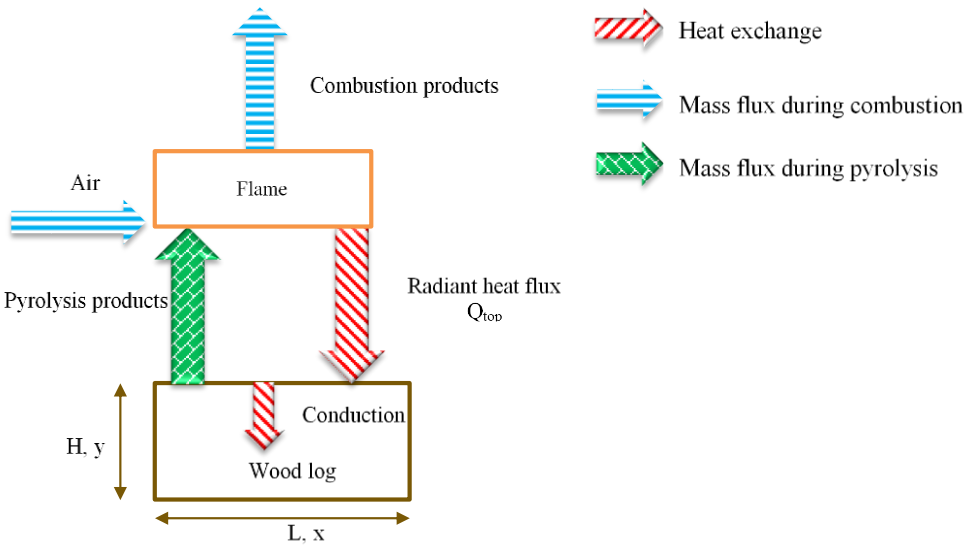

Fig.4. Main heat exchanges and mass fluxes occurring during the combustion of a wood log.

The study of heat transfer in a log of wood, considering the heterogeneity of this material as well as all the phenomena that can take place, is very complex. To simplify this problem, the following assumptions have been considered:

- The heat transfer according to the thickness and width of the log is assumed to be negligible: the resulting problem can be considered in 1D,
- The shape, mass, dimensions and physical properties of the log remain constant (m, λ_t, ρ, Cp ...),
- The convective heat transfer, which occurs between the volatile species produced during the pyrolysis and the solid residue, can be divided into natural convection and forced convection, and can be considered negligible due to the presence of air inlet which blow up the gas pyrolysis. This point will be investigated in future work.

According to these assumptions, the heat exchanges shown in Fig. 4 can be modelled by a heat conservation equation (1) coupled to boundary and initial condition limits represented by equations (2) and (3), respectively. The log is supposed to be initially at the inset temperature.

$$\rho Cp\frac{\partial T}{\partial t} - \lambda_t\left(\frac{\partial^2 T}{\partial y^2}\right) = 0 \quad (1)$$

$$\text{For } y = H, -\lambda_t\left(\frac{\partial T}{\partial y}\right) = Q_{top} = \varepsilon\sigma(T_f^4 - T^4(H,t)) \quad (2)$$

$$\text{At } t = 0 \text{ sec}, T(y,0) = T_{inset} \quad (3)$$

Equation (1) is a Partial Differential Equation (PDE) of second order, written in spatial coordinates. It is considered that only the upper layer of the log is reactive. The rest of the wood is supposed to be nonreactive when writing this heat balance. This allow decoupling the chemical (reaction enthalpy, which is considered in PSR 1) and physical phenomena (heat transfer) and obtaining equation (1) with only two terms. The first is a term of heat accumulation that characterizes the average heat capacity of wood. The second term describes the heat transfer by conduction according to Fourier's law.

The numerical resolution of the heat conservation equation coupled to the initial and boundary conditions is carried out by the software MATLAB® [31], using the Finite Element Method (FEM). Coupling heat transfer and chemical kinetic model is crucial to realize all the required simulations of the developed ERN, representing all processes during wood combustion.

III.2. Coupling between the thermal and kinetic model and iterative determination of the flame temperature

The coupling between chemical kinetics and heat transfer was achieved by coupling the two software CHEMKIN-PRO® and MATLAB®. As shown in Fig.5, this coupling aims to:

- Solve the thermal balance in the log in order to determine the average temperature of the layer on the log surface (T1),
- Model the reactors of the developed ERN by piloting the simulations carried out by CHEMKIN-PRO®,

- Exploit the results.

One of the main objectives of coupling chemical kinetics to heat transfer model is the determination of the flame temperature. This was achieved by applying energy balance in Chemkin, using an iterative resolution method developed between the output temperature of PSR-2 and the input temperature of PSR-1. This method is fully explained in Supplementary Material.

Once the flame temperature is determined, the simulation of all the elements of the constructed ERN (PSR-1→PSR-2→PFR-1→PSR-3→PFR-2→PFR-3) allows following the wood combustion process and determining the temperatures and the mole fractions of the gaseous products at the outlet of each reactor. The simulation of PFR-3, which represents the chimney, makes it possible to obtain the temperature and the composition of the combustion products.

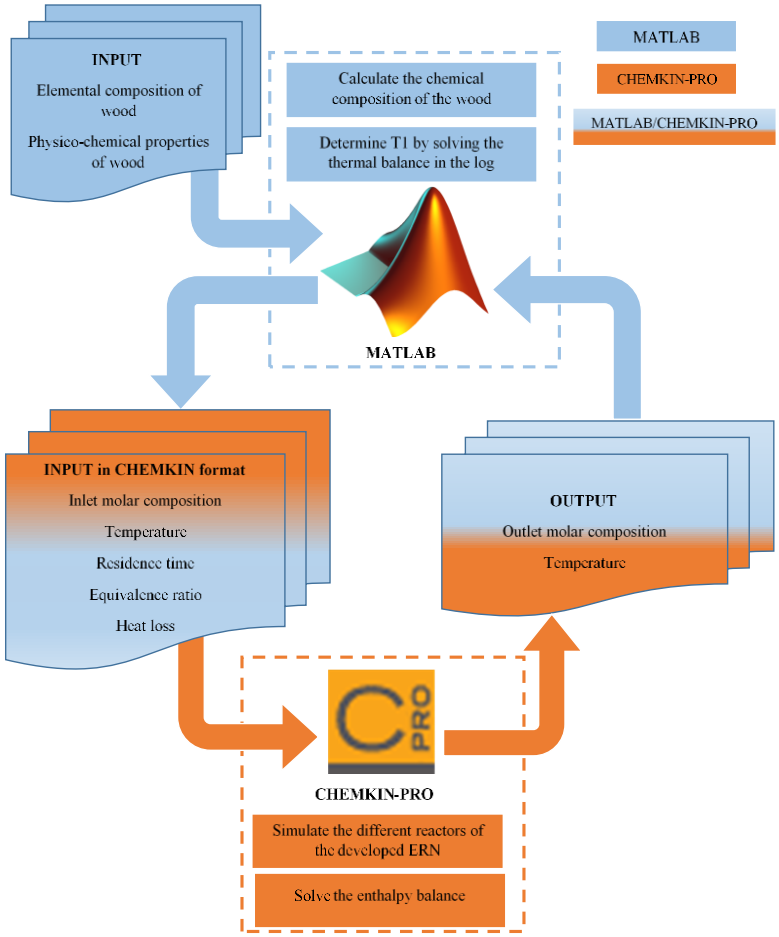

Fig.5. Coupling of two software CHEMKIN-PRO® and MATLAB®.

IV. Kinetic model update and validation with experimental results

The first part of BioPOx-1, as developed by Dhahak et al.[23], consists of the semi-detailed mechanism developed by Debiagi et al.[32] together with heterogeneous char combustion reactions according to what was proposed by Ranzi et al.[20]. According to the used primary pyrolysis model, the biomass is considered as a mixture of cellulose, hemicellulose and lignin. Reference species are chosen to represent each of these biomass constituents. The second part of BioPOx-1 model takes into account the decomposition of some species chosen as surrogates of tars produced by the pyrolysis of biomass. Models from the literature were considered for hydroxyacetaldehyde, furan and its derivatives, anisole, furfural and guaiacol (with a few up-

dated reactions compared to Weber et al.[17]), together with a detailed mechanism for the combustion of usual hydrocarbons and a mechanism for nitrogen oxides (NO_x) formation. BioPOx-1 model can simulate reasonably well results obtained in 19 experimental studies from the literature, for pyrolysis and combustion of key compounds of biomass pyrolysis, key compounds for Polycyclic Aromatic Hydrocarbons (PAH) formation and biomass and its constituents, for a wide range of operating conditions (equivalence ratios, temperatures and pressures)[23].

In order to improve the emission simulation as presented hereafter, an updated version of the BioPOx-1 model (named BioPOx-2) was proposed. Following are some examples of the main corrections and updates done to the kinetic model.

- Two intermediate species and 11 decomposition reactions were added in order to decompose the species (CH_2CCCHO), which was significantly overpredicted using BioPOx-1. Along with that, the simplified block of reactions of $CH_2CCHCHO$ was updated with a new version found in the model of Ranzi et al.[33]
- Because the levoglucosan (LVG) output results given by the simulation was dramatically lower than the experimental values, a series of reactions was added for the species $C_4H_6O_2$ and $C_6H_{10}O_5$.
- To better predict acetone formation, reactions producing the intermediate specie $CH_3(CO)CH_2$ were added.

As is shown in Figure 6, these changes only slightly affect the results that were obtained during the test of BioPOx-1.

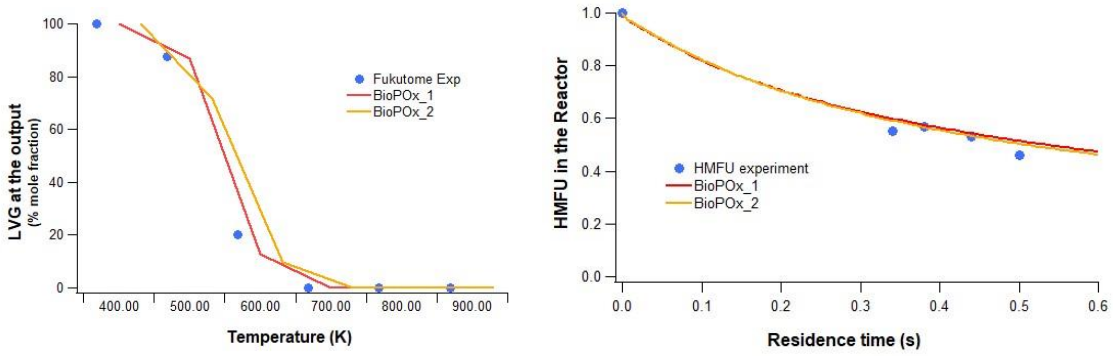

Fig.6. Effect of the kinetic changes on the previous tests of BioPOx-1: LVG pyrolysis at different constant temperatures as studied by Fukutome et al.[34], and hydroxymethylfurfural (HMFU) pyrolysis in a PFR at fixed temperature (650 K) as studied by Shin et al.[35]

As is shown in Figure 7, the above listed changes mainly affected two species: acetaldehyde and LVG.

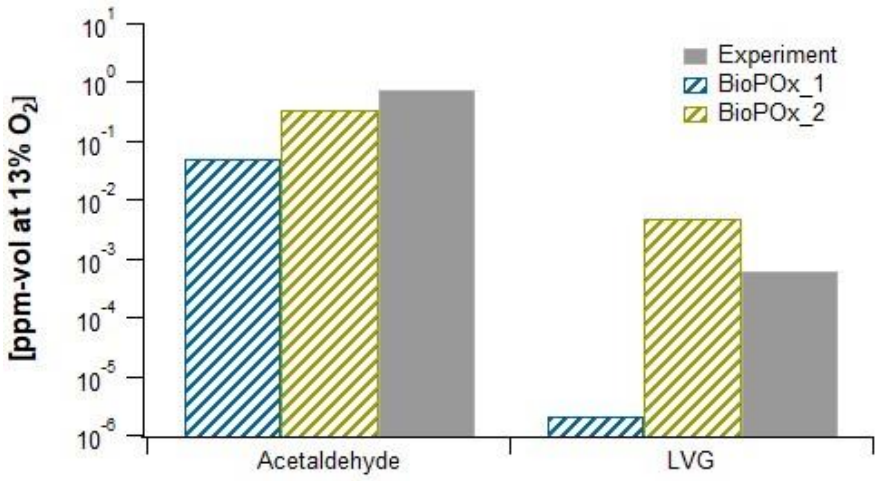

Fig.7. Influence of kinetic updates on the mole fraction (in log scale) of two emitted products at the outlet of the chimney during the combustion of hornbeam wood (Sample 2).

The BioPOx-2 is available in SM and involves 632 species and includes 4759 reactions.

V. Comparison of the model simulation against experimental results obtained on a wood inset

After describing the ways how the devolatilization mass flux and the ERN parameters have been obtained, this paragraph will present the used ERN model and a comparison between the gaseous emissions listed in part I.2 and the simulation results obtained from the ERN model with the thermal model (see part III.1) and the kinetic mechanism (see part III.2). A table presenting the simulation results is given in Supplementary Material with the formulae of the heavy species displayed in a second Table.

V.1. Determination of the mass flux produced through wood devolatilization

One of the key points of calculation is the determination of the mass flowrate of the pyrolysis products. To get an idea of this value, the following assumptions have been made:

- In the case of a log of hornbeam, the dimensions of the log lead to a volume of 0.00115395 m^3 (330 x π x 35^2)
- The density of the hornbeam is around 790 kg/m^3, therefore each log has an overall weight of 911.6 g
- The humidity of the hornbeam is 12.3% (as measured before the experiments), leading to a dry weight of wood around 799.5 g
- Considering a ratio Wood/Char of 90%, a mass of around 719.5 g of wood can be potentially pyrolyzed into gas
- Because, according to Fig. 2, one hour is needed to devolatilize the full wood log into gas and char, the overall mass flowrate can be taken equal to around 0.2 g/s.

The same type of calculation in the case of a densified wood or pine pallet leads also to a value around 0.2 g/s.

V.2. Parameters used in the reactor network (ERN)

Some parameters are related to the iterative method for determining the flame temperature: the initiation flame temperature T0 (taken as 2500 K) and the duration of exposure of the log to the flame (assumed to be of the order of 250 s). This last parameter corresponds to the minimum numerical time required to obtain a sufficient temperature in the upper layer of the log to produce the flame.

The other parameters correspond to the operating conditions of each element of the constructed ERN, as described in Table 2. The residence time in each reactor (τ), the equivalence ratio (ϕ) (in PSR-2 and PSR-3) and the heat losses were optimized to reproduce the experimental results in the case of the combustion of a log of hornbeam from sample 2. The mass flowrate in PSR-1 is the value calculated above (M=0.2 g/s). Knowing the composition exiting in PSR-1 (respectively PFR-1), the mass flowrates of primary air (Air-1) and secondary air (Air-2) are calculated in order to get the equivalence ratios given in Table 3.

The equivalence ratio is defined as: $\phi = \frac{(\frac{n_{fuel}}{n_{O_2}})_{real}}{(\frac{n_{fuel}}{n_{O_2}})_{stoich}}$

In our case, it can be written in the following form: $\phi = \frac{C_a H_b O_c N_d}{O_2}\ \alpha_{\text{stoich}}$

Air is modeled as a mixture of perfect gases containing 21% (mol) of O_2 and 79% (mol) of N_2. The stoichiometry is defined considering the general following chemical reaction:

$$C_aH_bO_cN_d + \alpha\ (O_2 + 3.76\ N_2) \rightarrow a\ CO_2 + \frac{b}{2}\ H_2O + \alpha_{stoich}\ N_2$$

with $\alpha_{stoich} = a + \frac{b}{4} - \frac{c}{2} + \frac{d}{2}$ and $\frac{O_2}{N_2} = \frac{0.21}{0.79}$

Table 3: Optimized parameters of the developed ERN.

Zone	Reactor	τ (sec)	ϕ [a]	Heat loss (Qloss) [b]	Dimensions		Temperature (°K) [c]	Pressure (atm)
					D (cm)	L (cm)		
Pyrolysis	PSR1	0.05	∞	1.5 cal/s	-	-	1400	1
Primary combustion	PSR2	0.0046	0.466	0	-	-	1200	1
Post-Combustion	PFR1	0.0001	0.03	0.533 cal/cm^2.s.K	1.8	0.15	1200	1
	PSR3	7	-	0	-	-	750	1
Deflector	PFR2	0.0314	-	0.2 cal/cm.s	1.8	30	750	1
Chimney Duct	PFR3	1.337	-	1.7 cal/cm.s	15	17	-	1

[a] Equivalence ratio. [b] Heat loss is expressed in cal/s for PSR and cal/(s.cm) for PFR. [c] Initial temperature, used to initiate the calculations.

Note that the residence time in PFR-1 is smaller than that in PSR-2. As shown in Figure 8, in PFR-1, not only temperature is decreased from above 1800 K to below 700 K, but also CO is rapidly converted to CO_2. With a larger residence time in PFR-1, too many CO is consumed in this PFR when reaching a reasonable exit temperature. The chosen values for the residence time and the heat-transfer coefficient are optimal to get a high enough decrease of temperature without an important loss of CO. These ERN parameters were adjusted to reproduce the experimental results of CO_2 concentration and the temperature of the combustion products in the case of the combustion of a log of hornbeam from sample 2.

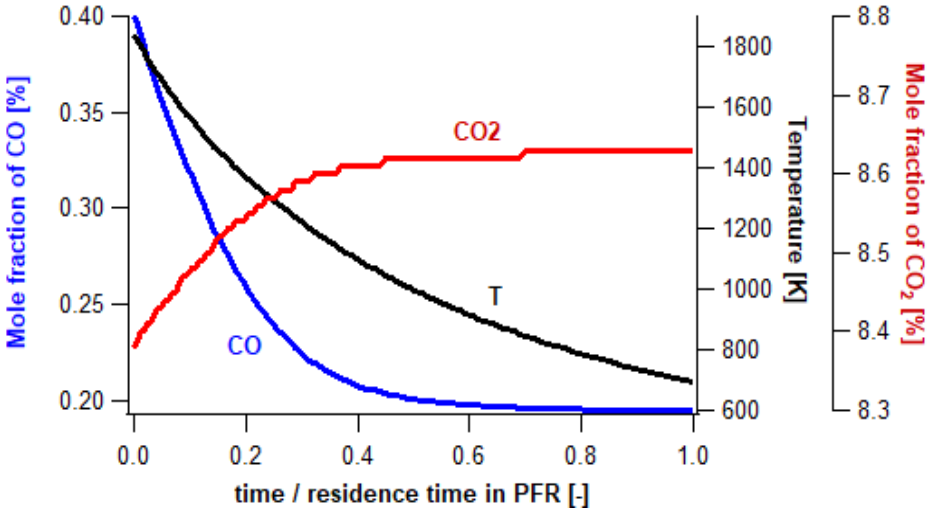

Fig.8. Time dependence of temperature and CO and CO_2 mole fraction in PFR-1.

The results of the study of Leclerc et al.[21] indicate an average residence time distribution of 11 seconds compared to 8 seconds obtained in this work. Considering that the two geometries of the insets were slightly different, we can consider that these two values are in good agreement.

Using the parameters summarized in Table 3, the predicted flame temperature obtained for the hornbeam log is 1920 K. This flame temperature is consistent with the results found in the literature. According to a study of Jenkins et al.[36], adiabatic flame temperatures from dry biomass combustion range from 2000 to 2700 K. Thornock et al.[37] studied the effect of adding different quantities of oxygen to biomass combustion. The shape, intensity and temperature of the flame were recorded using a two-color digital camera. The flame temperature obtained by adding 2 kg/h of oxygen is of the order of 2100 K. Panahi et al.[38] used a flame temperature of 2250 K in their particle-scale thermal model to study the combustion of miscanthus and beech wood. Liu et al.[39] studied the oxidation of gases derived from several biomasses. For pinewood, the flame temperature resulting from the combustion of the pyrolysis gases produced is 2119 K.

V.3. Comparison between simulated results and experimental measurements for pollutant emissions.

Thanks to the coupling of detailed kinetic mechanism to the heat transfer model, the flame temperatures obtained for the combustion of the different types of woods were determined. Using these temperatures, the simulation of all the elements of the developed ERN allowed following the pollutant emissions during the studied wood combustion. The emissions of CO, CO_2, NO and O_2, obtained by the model at the outlet of PFR-3, which represents the chimney, were compared to the experimental values in order to validate the developed tool. The modelling results were also compared to the mole fraction of PAHs, BTEX (Benzene, Toluene, Ethylbenzene, Xylenes) and levoglucosan (LVG) measured in the chimney. In this paragraph,

the results of the hornbeam combustion of Sample 2 is presented first for all quantified species, followed by a comparison between all the samples results tested both experimentally and numerically for selected species. The simulation results for all species and all samples are given in the spreadsheet in SM. The experimental results correspond to the averages of the results obtained during two tests performed during nominal phases (nominal 1 and nominal 2: Fig.2). No further parameter adjustment (compared to Table 3) was performed.

a. CO, CO_2, NO_X and O_2 emissions

Table 4 shows the comparison between numerical and experimental results for the mole fractions of CO, CO_2, O_2 and NO_X. The good agreement between experimental and numerical results of CO_2 and the temperature of the combustion products is directly linked to the fact that the ERN parameters were adjusted on these experimental results (as explained in V.2). Note that by using the model from a recent study by Song et al.[40], the simulated NO_X mole fraction is close to the experimental one obtained with hornbeam logs, despite the fact that the reactions of nitrogen present in the initial composition of wood was not considered.

Table 4: Mole fractions of CO, CO_2, O_2 and NO_X at the chimney outlet (PFR-3).

Mole Fraction (%)	**Hornbeam (Sample 2)** (used for optimization purpose)	
	Experimental	**Model**
O_2	13.4	12
CO*	0.19	0.306
CO_2	7.6	7.43
NO_X	2.40×10^{-3}	2.55×10^{-3}
Temperature [°C] of the combustion products	339	339

*Corrected at 13% O_2

b. Aldehydes, ketones and BTEX emissions

In Figure 9, BTEX (benzene, toluene, ethylbenzene and xylene) and aldehydes and ketones results obtained from the numerical combustion of hornbeam wood, are compared to the corresponding experimental results. Error bars correspond to the experimental uncertainties.

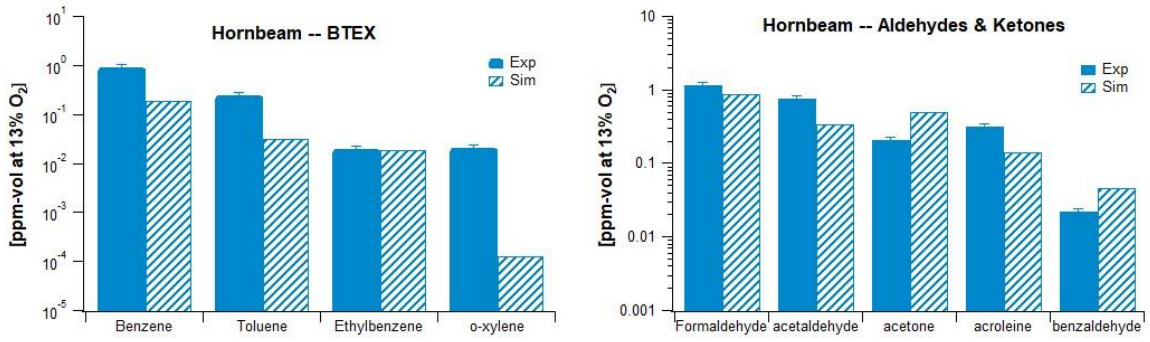

Fig.9. Mole fraction (in log scale) of BTEX, aldehydes and ketones at the outlet of the chimney (PFR-3) during the combustion of hornbeam wood (sample 2): comparisons between experimental and simulated results (corrected at 13% O_2).

The model allows simulating in a very acceptable way, the mole fractions of most of the BTEX and of all the main aldehydes and ketones shown in Figure 9. However, simulations under-predict the formation of xylene and under-predicts the formation of ethylbenzene.

c. PAHs, phenolic compounds and LVG emissions

Figure 10 shows the comparison between the experimental and numerical results of the mole fractions of some PAHs (naphthalene, phenanthrene, chrysene and pyrene), phenolic compounds (phenol, guaiacol and syringol) and LVG, for the combustion of hornbeam logs (sample 2). Error bars correspond to the experimental uncertainties.

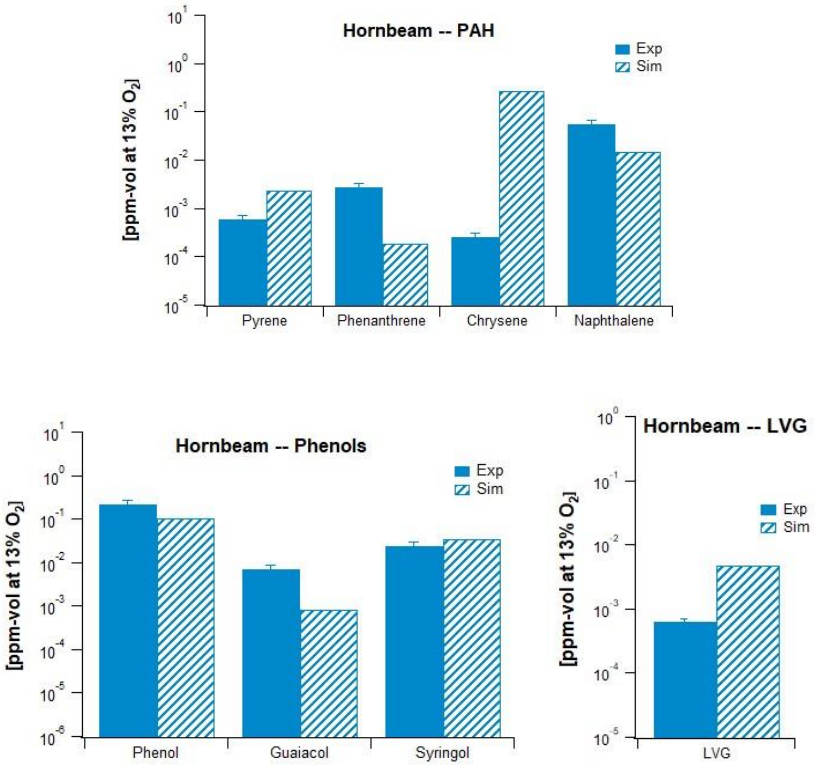

Fig.10. Mole fraction (in log scale) of some PAHs, phenols species and LVG at the outlet of the chimney (PFR-3) during the combustion of hornbeam woods: comparisons between experimental and simulated results (corrected at 13% O_2).

The model simulates quite satisfactorily (better than a factor of 10) the mole fraction of LVG, pyrene, phenanthrene, naphthalene and phenol, but over-predicts that of chrysene.

Overall, the agreement between experimental and simulated results is good for a wide range of pollutants in the case of hornbeam (Sample 2), for which the ERN parameters were only adjusted in order to fit the simulated outlet temperature and CO_2 mole fraction. The next paragraph will show the results for the other samples.

V.4. Simulation results for the full set of studied wood samples

The chemical composition of the seven considered samples is shown in Table 1. The difference in composition between these wood samples is not significant enough to be used to derive the sensitivity of result changes. The sensitivity on the wood composition affected the

experimental results more than it affected the numerical simulations. This is illustrated by the set of results shown in Figure 11. Error bars correspond to the experimental uncertainties. This can be due to the many factors that cannot or were not taken into account numerically, for example, the initial fraction of sulfur and nitrogen in the wood log, the presence or absence of bark or pretreatment (washing) of the wood and its impact on how the wood ignites/burns, the time-dependent variations (such as evolution of the draft within the chimney).

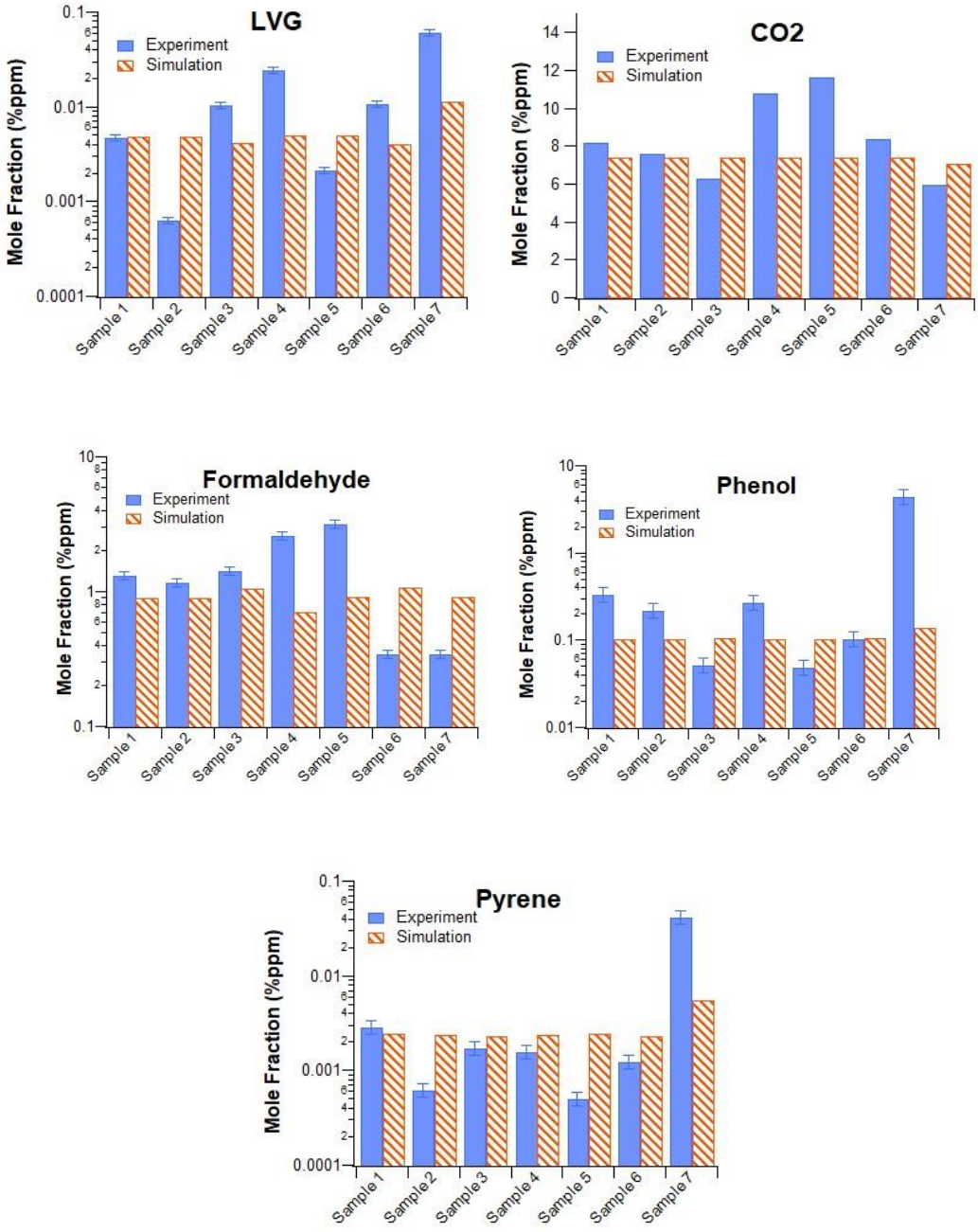

Fig.11. The spread of the results at the outlet of the chimney (PFR-3) during the combustion of the 7 samples shown in Table 1. The values are shown in mole fraction percentage for 5 of the important output species: LVG, CO_2, formaldehyde, phenol and pyrene

VI. A priori prediction of the variation of temperature and the mole fraction of important pollutants at different levels in the ERN

Thanks to the developed model, several information about the evolution of temperatures and the mole fractions of the major gaseous pollutants along the ERN can be provided.

VI.1. Temperature

The simulated evolution of the temperature at the outlet of each zone during the combustion of hornbeam (sample 2) is represented in Figure 12. These temperatures were derived from enthalpy balance in each ERN component. The outlet temperature of PSR-2 represents the flame temperature, which is the temperature right above the burning surface of the log (this temperature is higher than the one measured inside the visible flame). After leaving this zone (PSR-2), the temperature decreases rapidly along the inset.

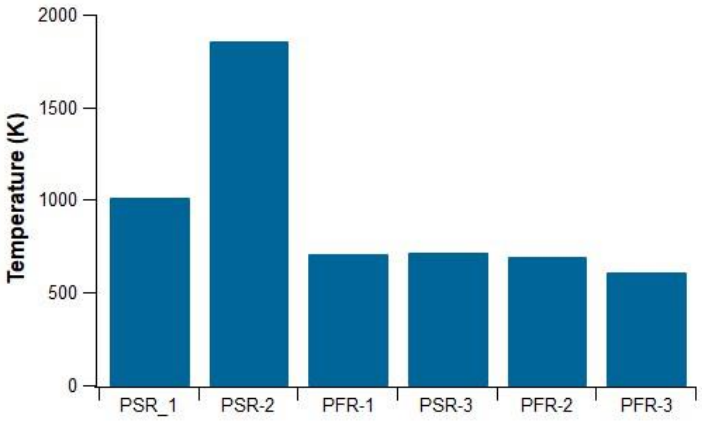

Fig.12. Evolution of the temperature at the outlet of each reactor during the combustion of hornbeam wood (sample 2).

VI.2. Important gaseous pollutants

The detailed kinetic mechanism BioPOx-2 was built in order to predict the formation and the evolution of several families of pollutants such as CO, CO_2, soot precursors, phenolic compounds (phenol, guaiacol ...), aldehydes (acetaldehyde, formaldehyde ...), ketones, and tracers of wood combustion (levoglucosan (LVG), hydroxyacteldehyde (HAA), hydroxymethlfurfural (HMFU)). Therefore, *a priori* prediction of the evolution along the ERN of the amount of these pollutants are shown hereafter. Two air supplies were considered, at the inlet of both PSR-2 and PFR-1 and the mole fractions of N_2 at the outlet of these reactors are about 70%. Considering the large N_2 mole fraction, a percentage of the total amount of carbon species at the outlet of each zone is plotted for each of the species mentioned in this part.

a. CO and CO_2

The evolution of the mole fractions of CO and CO_2 at the outlet of each zone is plotted in Figure 13. Figure 13 shows that there is a significant formation of carbon oxides (about 50% of CO and 11% of CO_2) nearby the combustion of the wood log. CO starts to be consumed in the flame reactor, PSR-2, and is almost fully destroyed in the post-combustion zone (PFR-1) to produce CO_2. It seems that after PFR-1 the global reactivity is very low, as the concentrations of CO and CO_2 remain constant. More generally, the same behavior is observed for the other compounds, such as naphthalene, toluene.... Therefore, while it has an important mechanical impact in controlling residence times, it seems that on a pure chemical point of view, the deflector zone (PFR-2+PFR-3) has a very limited influence.

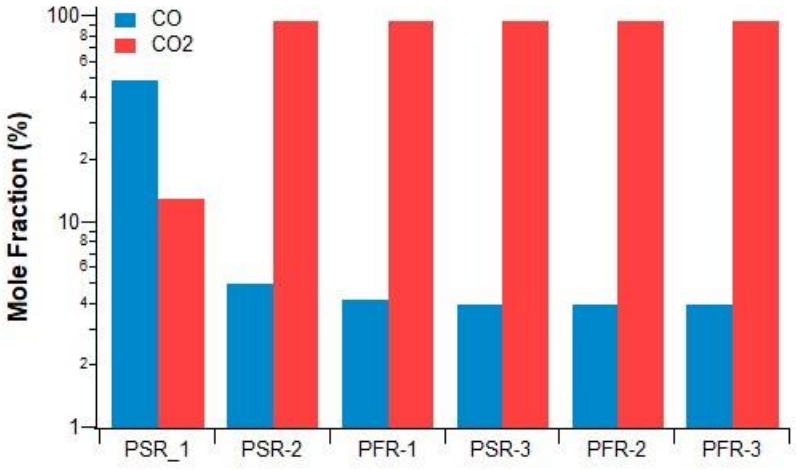

Fig.13. Evolution of the mole fractions of CO and CO_2 (in log scale) at the outlet of each reactor during the combustion of hornbeam wood (sample 2).

b. PAHs (soot precursors) & BTEX

One of the major problems of wood combustion is the formation of soot particles, which can be related to the formation of PAHs, considered as soot precursors. Indeed, the nucleation and coalescence of these cyclic molecules, having significant molecular weights, can cause the formation and growth of soot particles. Figure 14 shows the evolution of the mole fractions of some soot precursors (naphthalene, pyrene, and phenanthrene) and BTEX (benzene, ethylbenzene and toluene). A significant formation of aromatic species, especially benzene, is observed in the pyrolysis reactor (PSR-1). The degradation of these molecules (PAHs and BTEX) starts in the oxidation reactor (PSR-2) and continues in the post-combustion reactor, PFR-1. The mole fractions of all these species decrease significantly from PSR-2 to PFR-1. Hence, this confirms the interest of the post-combustion zone, which burns the residual volatile compounds.

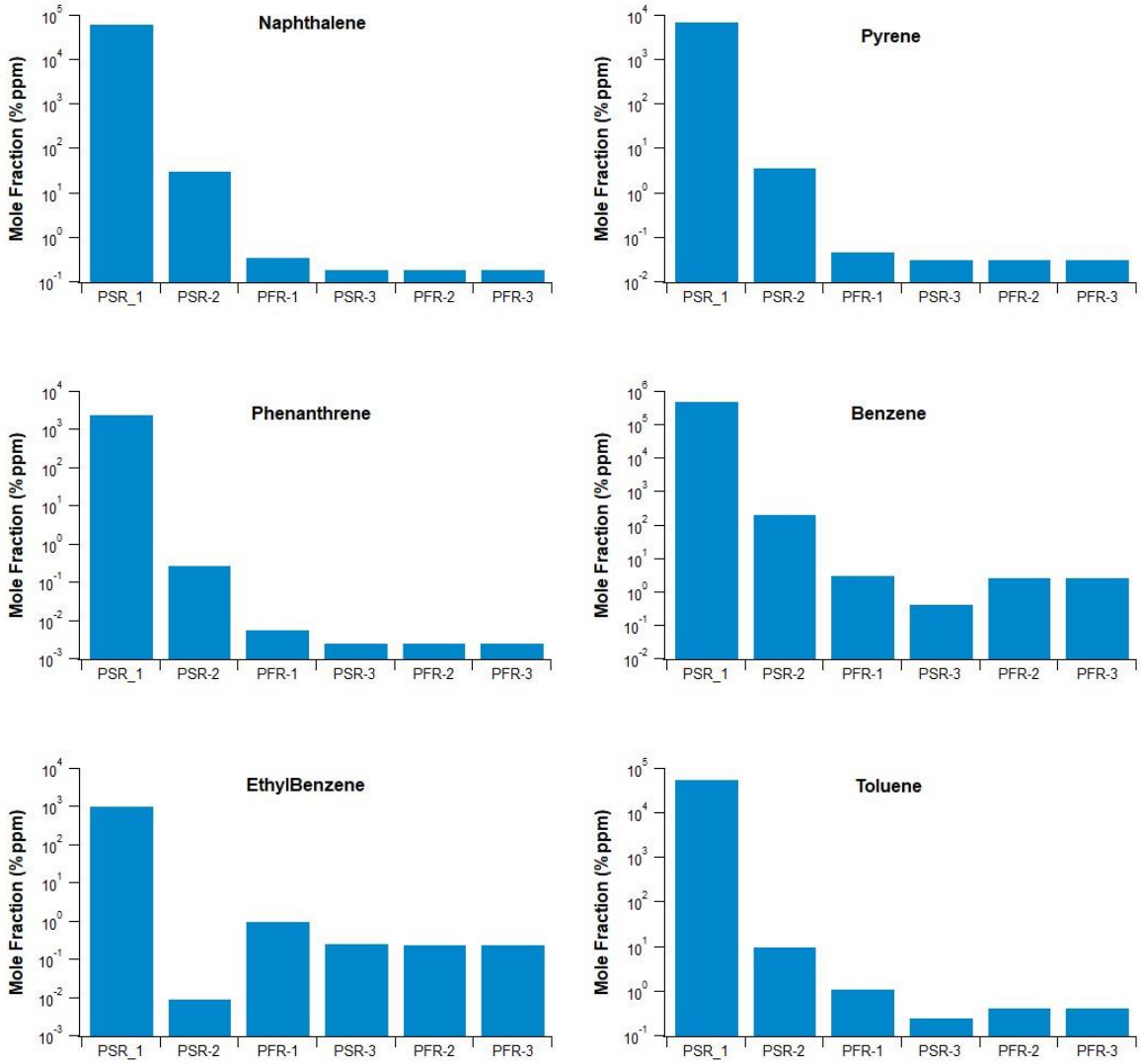

Fig.14. Evolution of the mole fractions (in log scale) of some PAHs (naphthalene, pyrene and phenanthrene) and BTEX (benzene, ethylbenzene and toluene) as a percentage of the total amount of carbon species at the outlet of each reactor during the combustion of hornbeam logs (sample 2).

c. Phenolic compounds

As shown in Figure 15, phenol is formed in the pyrolysis reactor (PSR-1) as a primary product of lignin degradation. Its consumption starts in the flame reactor (PSR-2) and continues (in a lesser extend) in the post-combustion zone (PFR-1). Unlike aromatic hydrocarbons, the

mole fractions of guaiacol and pyrocatechol increases after the combustion zone (PFR-1), since the lower temperature favors their formation by radical combinations and essentially the reverse bimolecular initiation with oxygen (see Fig. 16), involving the abundant OOH radicals.

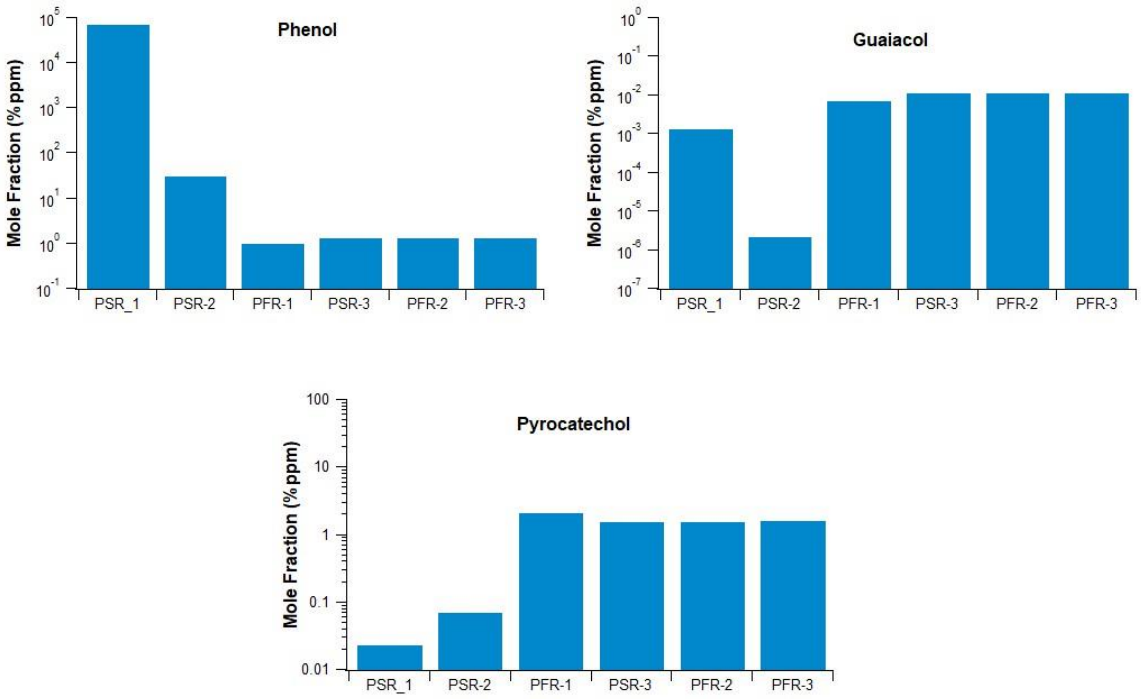

Fig.15. Evolution of the mole fractions (in log scale) of phenolic compounds (phenol, guaiacol and pyrocatechol) as a percentage of the total amount of carbon species at the outlet of each reactor during the combustion of hornbeam logs (sample 2).

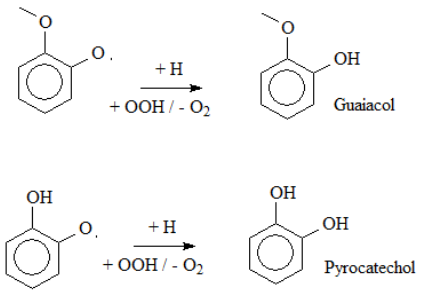

Fig.16. Reactions leading to guaiacol and pyrocatechol.

d. Aldehydes and ketones

The emissions of aldehydes (formaldehyde, acetaldehyde, benzaldehyde and acrolein) and ketones (acetone) are represented on Figure 17. All these compounds are formed in PSR-1 and mainly consumed in PSR-2 and PFR-1.

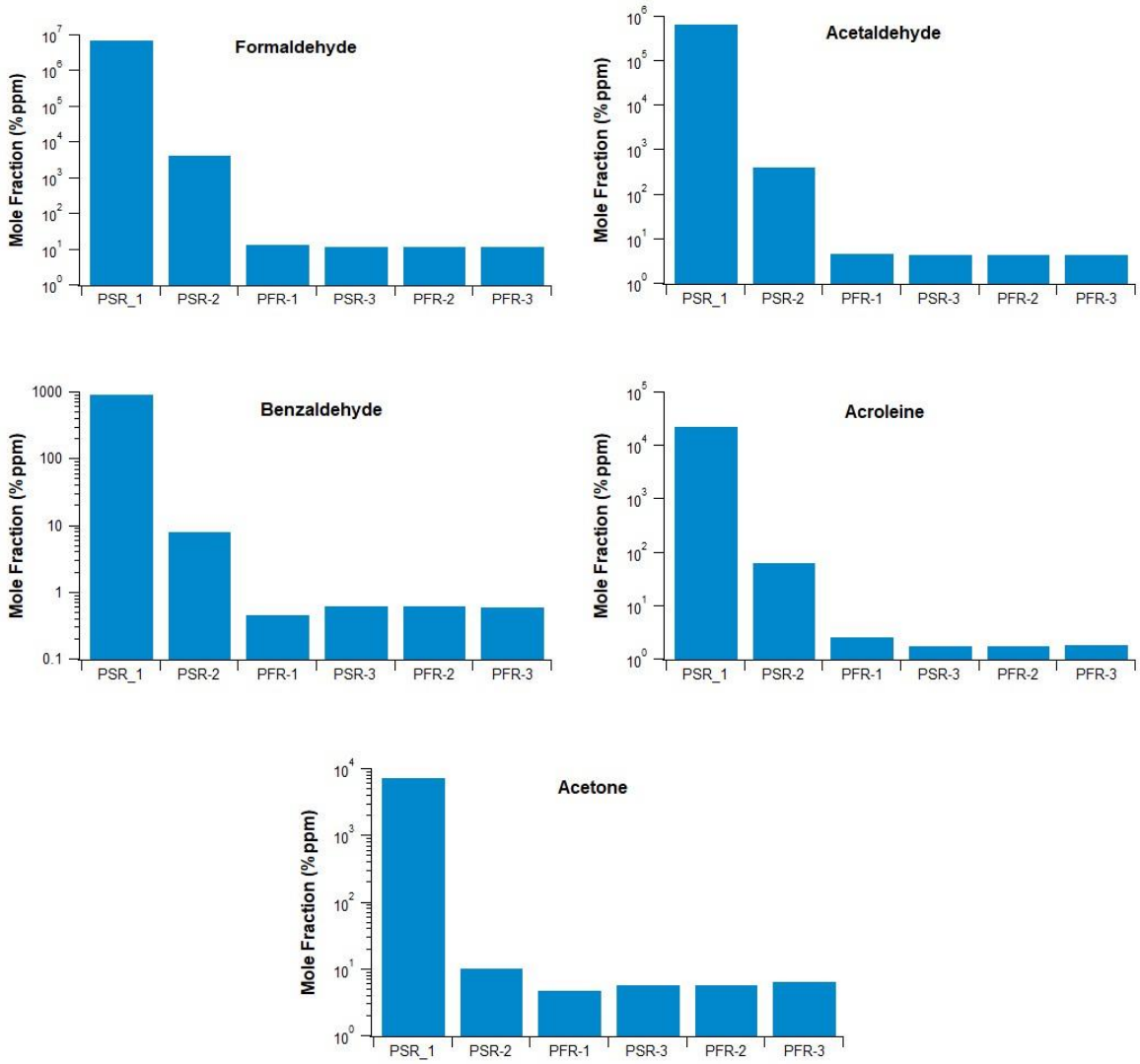

Fig.17. Evolution of the mole fractions (in log scale) of (formaldehyde, acetaldehyde, benzaldehyde and acrolein) and ketones (acetone) as a percentage of the total amount of carbon species at the outlet of each reactor during the combustion of hornbeam logs (sample 2).

e. Tracers of wood combustion

Figure 18 shows the evolution of the mole fractions of some key biomass pyrolysis compounds, such as levoglucosan (LVG), hydroxyacetaldehyde (HAA) and hydroxymethylfurfural (HMFU), at the outlet of different reactors considered in the ERN. Again, all these compounds are formed in PSR-1 and mainly consumed in PSR-2 and PFR-1.

After the secondary combustion in PFR-1 and PSR-3, there is no more chemical effect of PFR-2 and PFR-3.

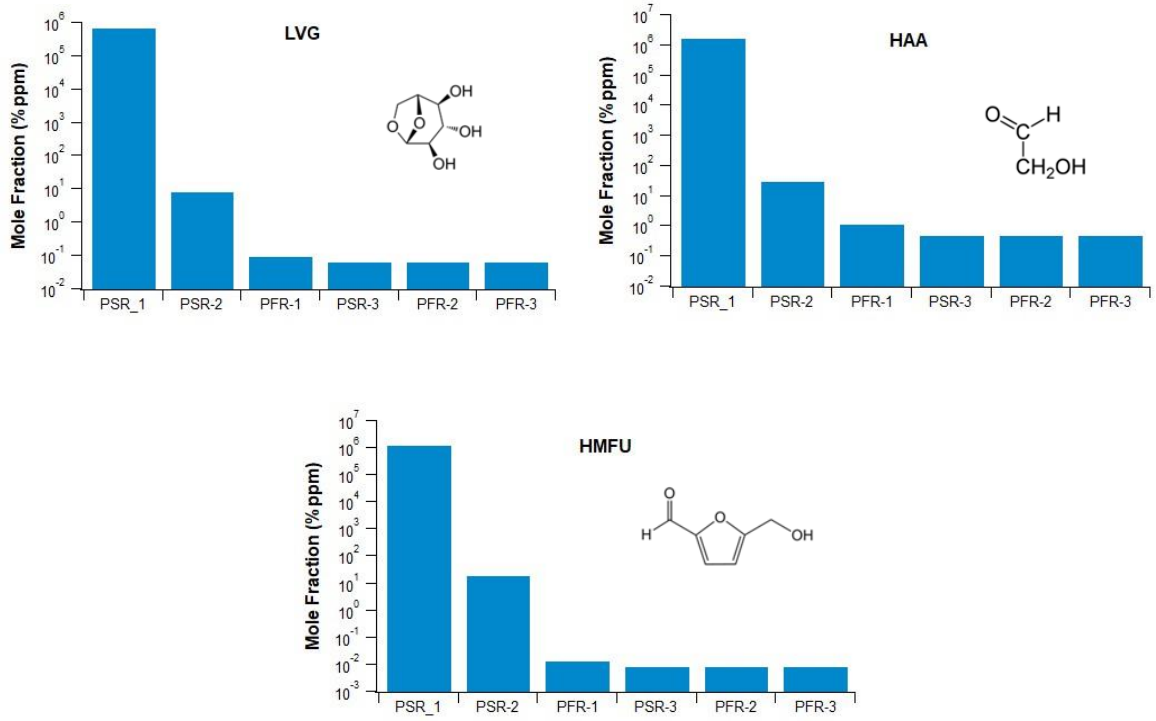

Fig.18. Mole fractions (in log scale) of key biomass pyrolysis compounds (LVG, HAA and HMFU) as a percentage of the total amount of carbon species at the outlet of each reactor during the combustion of hornbeam logs (sample 2).

VI.3. Sensitivity analysis of the ERN model

In order to investigate the influence of the ERN parameters on the flame temperature and the pollutant emissions, a sensitivity study using the Morris approach was conducted. The used

wood was hornbeam (sample 2), that on which the parameters were adjusted. The results of the parametric analysis show that most of the parameters, in particular the residence times, have nonlinear effects on the flame temperature and on the outlet mole fractions of CO, CO_2 and O_2. Based on these primary results, we have used an OFAT approach (One Factor at a Time) in our model for sensitivity analysis. OFAT is a local sensitivity analysis approach; it gives elementary effects and variances for the input parameters, which helps in identifying the most influencing parameters.

Three parameters were studied, the residence time in PSR-2, the primary air mass flow rate that enters PSR-2 and the secondary air mass flow rate that enters PFR-1. The mass flow rate of air is related to the equivalence ratio.

a. Effect of residence time

The residence time of PSR-2 has been varied from $2.4x10^{-3}$ to $1.0x10^{-2}$ s (reference value = $4.6 x10^{-3}$ s). The results are shown in Fig.19.

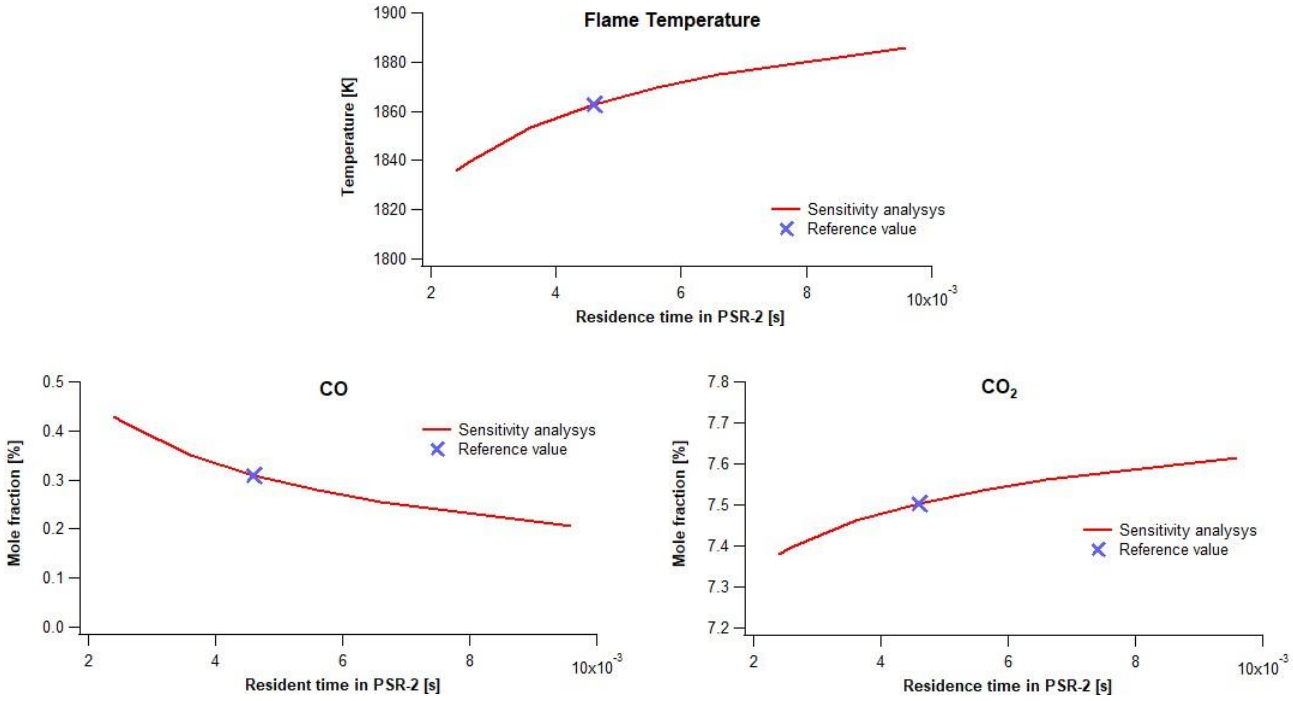

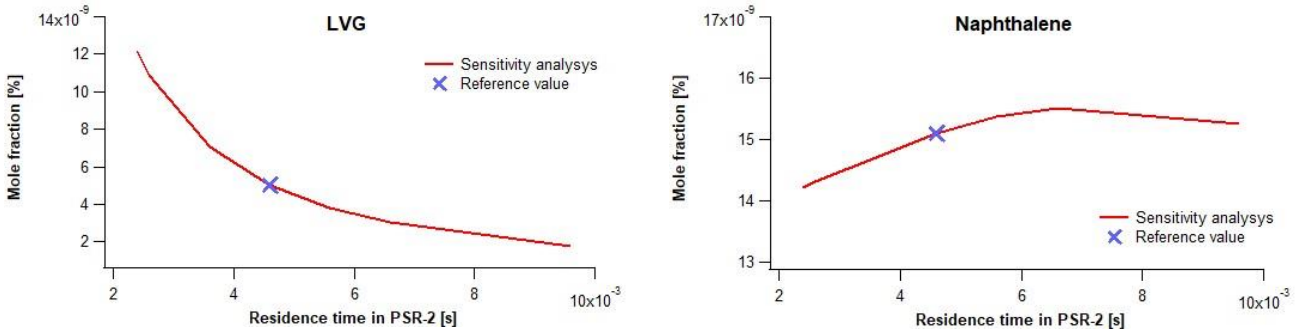

Fig.19. OFAT sensitivity analysis. Effect of varying the residence time in PSR-2 on the flame temperature and the mole fraction of representative species (hornbeam logs - sample 2).

This figure clearly shows an important increase of the flame temperature (the temperature at the outlet of PSR-2) when increasing this residence time. This temperature effect mostly explains that, when increasing the residence time in PSR-2, the mole fraction of CO_2, naphthalene and NO increases, whereas that of CO, toluene and LVG decreases, as is also shown in Fig.19.

b. Effect of primary air mass flow rate

As is shown in Figure 20, the PSR-2 outlet temperature decreases when the inlet airflow rate in this PSR increases from 0.4 to 2 g/s (reference value = 0.93 g/s), which correspond roughly to a variation of equivalence ratio from 1.5 to 0.2. As shown by OFAT, the primary air flowrate has an important effect on the flame temperature. At 0.4 g/s of air, the flame temperature is around 2400 K, this value decreases to 1325 K with an airflow of 2 g/s. For 4 g/s, the calculation leads to a flame temperature of around 770 K. This very low temperature means that no flame is observed, showing that no combustion occurs with a too high air flowrate.

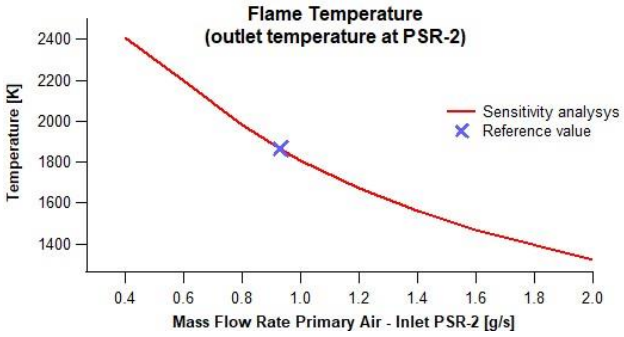

Fig.20. OFAT sensitivity analysis. Effect of primary air mass flow rate on the flame temperature (hornbeam logs - sample 2).

Figure 21 represents the variation of mole fraction of CO, CO_2, NOx, LVG, toluene and naphthalene in function of flame temperature (the temperature in PSR-2) varied by changing the primary air flowrate. This figure leads us to the following strategy: it is necessary to obtain a high enough flame temperature in order to decompose the PAHs compounds (symbolized by naphthalene) but not too high in order to avoid a too high formation of CO and NOx compounds. It seems that a flame temperature around 1800K was a good compromise.

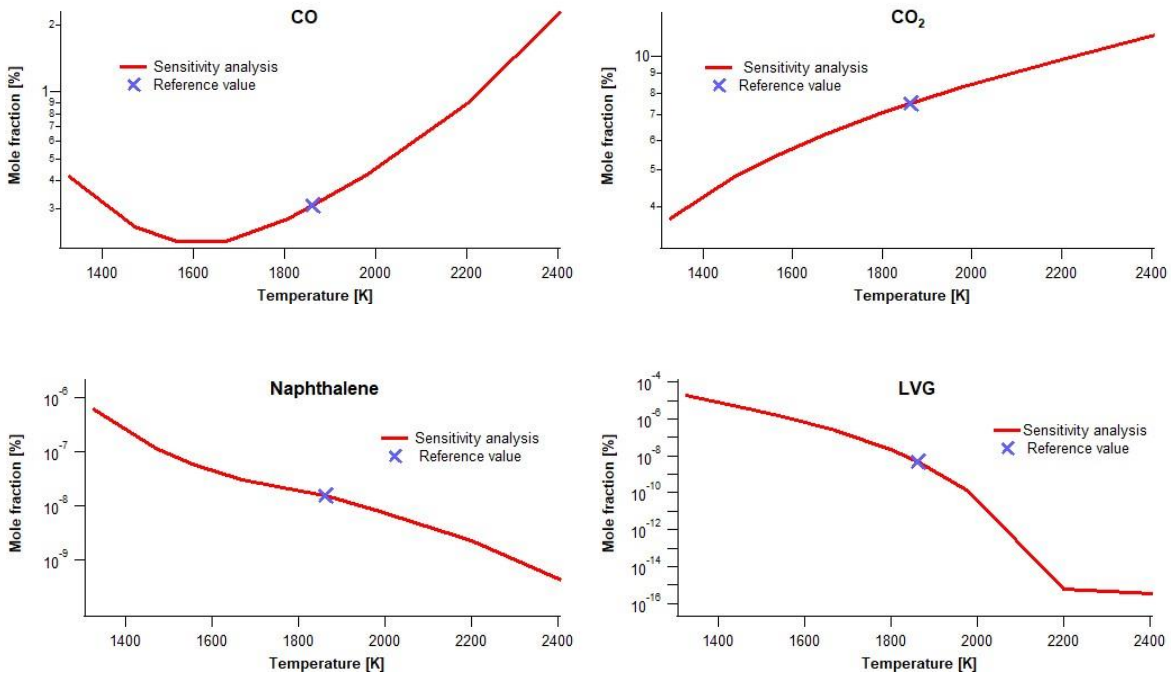

Fig.21. OFAT analysis. Effect of a variation of the flame temperature obtained by varying the primary air mass flow rate, on the mole fraction of CO, CO_2, naphthalene, and LVG (hornbeam logs - sample 2).

c. Effect of secondary air mass flow rate

To better understand the effect of the secondary combustion, the airflow rate in PFR-1 was varied from 0 to 0.4 g/s (reference value = 0.2 g/s). A decrease in the mole fractions of the main pollutants is observed when the secondary air flowrate is increased. The effect on toluene is shown in Figure 22. This shows well the positive influence of secondary combustion for reducing the formation of the precursors of PAHs and soot.

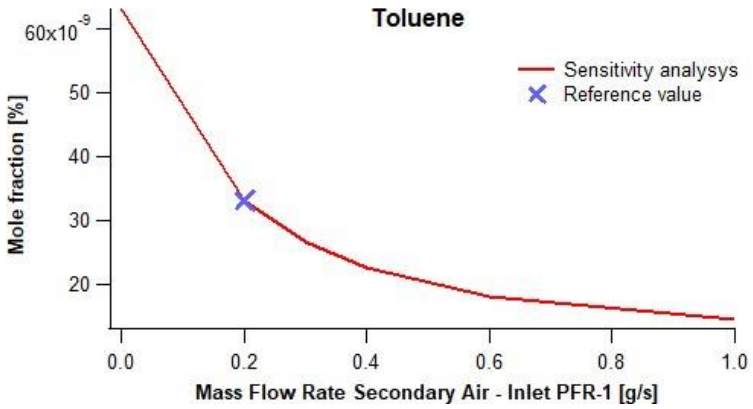

Fig.22. OFAT sensitivity analysis. Effect of secondary air mass flow rate on the mole fraction of toluene (hornbeam logs - sample 2).

d. Effect of the pyrolysis of the devolatilization products in PSR 1

During the previous part of this study, all simulations were performed with the full BioPOx model including both the devolatilization reactions (primary pyrolysis) and the gas-phase reactions of the produced volatile species, which involve that in PSR-1 gas-phase secondary pyrolysis occur in parallel to solid phase reactions. The effect of considering both pyrolysis mechanisms is investigated hereafter.

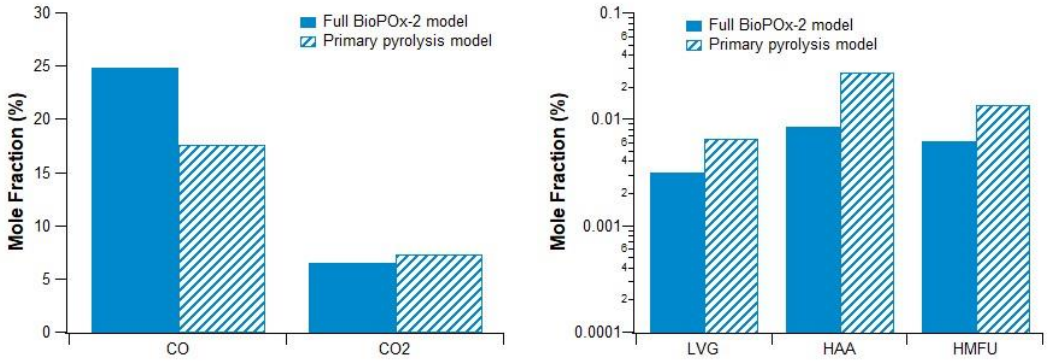

Fig.23. Effect of the used model (only the primary pyrolysis model or the full BioPOx-2 model) on the pyrolysis products obtained at the outlet of the pyrolysis reactor (PSR-1) during the combustion of hornbeam logs (sample 2). Shown in normal scale for CO and CO_2 and in log scale for LVG, HAA and HMFU.

As shown in Figure 23, about 30% of the amount of CO obtained at the outlet of PSR-1 is formed by pyrolysis of the species from solid devolatilization. Some other primary pyrolysis products, such as LVG, HAA and HMFU, already decompose in PSR-1 by thermal cracking reactions to form lighter products.

Conclusion

Optimizing wood combustion in domestic heating appliances requires a better understanding of the chemistry of the formation of pollutants and the physical phenomena, such as heat transfer, during combustion in such equipment. In this work, we developed a simplified global model of wood combustion in a domestic inset using an Equivalent Reactor Network (ERN) approach. The studied heating appliance was represented by six ideal reactors representing both the devolatilization of the biomass and the combustion of the released gaseous species.

This simplified ERN approach allowed us to consider a very detailed chemistry, using the kinetic model, BioPOx-2, which involves 632 species and includes 4759 reactions. This model

was coupled to a simplified heat transfer model to represent the combustion of a wood log in an inset. The thermal model developed on the scale of the log, allows determining the profile of the temperature in the different layers of the log, from the surface to the depth. Coupling the kinetic model BioPOx-2 to the thermal model was made by coupling the software MATLAB® and CHEMKIN-PRO® to solve the thermal balance in the wood log, in order to determine the flame temperature and to obtain the temperatures and the chemical compositions at various points of the developed ERN.

Simulations using the global model were compared to experimental results obtained for 7 batches of wood in a wood inset, in which pollutant emissions were followed within the chimney. Some parameters of the ERN, such as residence times, equivalence ratios and heat losses, were optimized in the case of the combustion of a sample of hornbeam. Using these same parameters, the agreement between the experimental results and those of the model were acceptable for the wide range of measured pollutants, including mono-aromatic, carbonyl and phenolic compounds, as well as polycyclic-aromatic hydrocarbons (PAHs) and sugars. Furthermore, the level of agreement remained acceptable for the combustion of the other wood samples. This new model allows a first rough calculation of the temperature and the mole fractions of the main expected gaseous pollutants in each reactor of the ERN.

This work should only be considered as a very first attempt for predicting pollutant emissions from a domestic heating appliance and many points need to be improved in terms of kinetic model of biomass combustion, heat transfer model and ERN model. In the future, the tool developed and improved might be used to predict and optimize wood combustion according to three possible scenarios:

- First, by fixing the wood type and looking for the "ideal" operating conditions of the heating appliance that ensure a good compromise between the thermal efficiency and pollutant emissions;

- Second, by setting the operating conditions and looking for the "ideal" wood type to guarantee a good compromise between thermal efficiency and pollutant emissions.
- Third, by fixing the wood type and the operating conditions and optimizing the airflow within the inset (through the use of other more complex configurations of ERN) to ensure a good compromise between the thermal efficiency and the pollutant emissions.

In the mid-term, a coupling with a soot model might allow predicting particle formation, as the present model can already predict the emissions of large species like pyrene, the basic bloc in the formation of soot particles in many models from literature[41 42].

Moreover, improvements of the simulation process will be envisaged through studies focusing on different aspects and considering:

- the effects of radiation and thermal transport.
- a better estimation of heat losses.
- a more detailed NOx study.
- a more accurate method to evaluate residence times.
- the effects of recirculation and mass transport.
- the improvement of the ERN to better simulate the process.
- the effects of the changing specific heat (Cp), mass and other properties of a wood log during the combustion process.

Acknowledgment

The authors gratefully acknowledge *the Agence de la transition écologique* (ADEME) for the financial support of this work as well as Sylvain AGUINAGA from CSTB, Gwenaëlle TROUVE from LGRE, Dorothée DEWAELE and Coralie PUSCA from CCM and Fabien

BALAY and Frédéric ROBIC from the LORFLAM company for their collaboration within this project.

Supplementary Material

Supplementary Material associated with this article can be found in the online version:

- Detailed kinetic mechanism in Chemkin format: *BioPOx-2 meca.txt*
- Thermo file for the mechanism: *BioPOx-2 thermo.txt*
- A file containing the experimental data, experimental measurements uncertainties, explanations on the methods of determination of the flame temperature and the simulation results: *Supplementary Material.pdf*

References

(1) UNECE. *Wood Energy in the ECE Region*; **2017**, iii (3-4). https://unece.org /DAM/timber/publications/SP-42-Interactive.pdf

(2) World Meteorological Organization. WMO Greenhouse Gas Bulletin. *WMO Bull.* **2020**, No. 16, 1-9. https://library.wmo.int/doc_num.php?explnum_id=10437

(3) Internation Energy Agency (IEA), Net Zero by 2050 A roadmap for global energy sector, **2021**, 90-94 , www.iea.com.

(4) Camia A., Giuntoli, J., Jonsson, R., Robert, N., Cazzaniga, N.E., Jasinevičius, G., Avitabile, V., Grassi, G., Barredo, J.I., Mubareka, S., The use of woody biomass for energy production in the EU. *JRC science for policy report*. **2021,** 9**.** https://www.eia.gov/energyexplained/biomass/biomass-and-the-environment.php

(5) Chiffres Clés Des Énergies Renouvelables Édition 2020. *Le Service des données et études statistiques (SDES) Chiffres*. **2020**, 5-20, https://www.statistiques.developpement-durable.gouv.fr/chiffres-cles-de-lenergie-edition-2020-0 .

(6) Alison S. Tomlin, Air Quality and Climate Impacts of Biomass Use as an Energy Source: A Review. *Energy and Fuels* **2021**, 35, 14213-14240.

(7) Tschamber V., Trouvé G., Leyssens G., Le-Dreff-Lorimier C., Jaffrezo J. L., Genevray P., Dewaële D., Cazier F., Labbé S., Postel S., Domestic Wood Heating Appliances with Environmental High Performance: Chemical Composition of Emission and Correlations between Emission Factors and Operating Conditions, *Energy&Fuels*, **2016**, *30* (9), 7241-7255

(8) Schmidt G., Trouvé G., Leyssens G., Schönnenbeck C., Genevray P., Cazier F., Dewaële D., Vandenbilcke C., Faivre E., Denance Y., Le Dreff-Lorimier C., Wood washing: Influence on gaseous and particulate emissions during wood combustion in a domestic pellet stove, *Fuel Processing Technology*, **2018**, *174*, 104-117

(9) Andersson, J.; Umeki, K.; Furusjö, E.; Kirtania, K.; Weiland, F. Multiscale Reactor Network Simulation of an Entrained Flow Biomass Gasifier: Model Description and Validation. *Energy Technol.* **2017**, *5* (8), 1484–1494. https://doi.org/10.1002/ente.201600760.

(10 Lu, H.; Robert, W.; Peirce, G.; Ripa, B.; Baxter, L. L. Comprehensive Study of Biomass Particle Combustion. *Energy and Fuels* **2008**, *22* (4), 2826–2839. https://doi.org/10.1021/ef800006z.

(11) Yang, Y. B.; Sharifi, V. N.; Swithenbank, J.; Ma, L.; I, L.; Jones, J. M.; Pourkashanian, M.; Williams, A.; Darvell, L. I. Combustion of a Single Particle of Biomass. *Energy & Fuels* **2008**, *22* (8), 306–316. https://doi.org/10.1021/ef700305r.

(12) Haberle, I.; Skreiberg, Ø.; Łazar, J.; Haugen, N. E. L. Numerical Models for Thermochemical Degradation of Thermally Thick Woody Biomass, and Their Application in Domestic Wood Heating Appliances and Grate Furnaces. *Prog. Energy Combust. Sci.* **2017**, *63*, 204–252. https://doi.org/10.1016/j.pecs.2017.07.004.

(13) Porteiro, J.; Collazo, J.; Patiño, D.; Granada, E.; Gonzalez, J. C. M.; Míguez, J. L. Numerical Modeling of a Biomass Pellet Domestic Boiler. *Energy and Fuels* **2009**, *23* (2), 1067–1075. https://doi.org/10.1021/ef8008458.

(14) Tabet, F.; Fichet, V.; Plion, P. A Comprehensive CFD Based Model for Domestic Biomass Heating Systems. *J. Energy Inst.* **2016**, *89* (2), 199–214.

https://doi.org/10.1016/j.joei.2015.02.003.

(15) Kausley, S. B.; Pandit, A. B. Modelling of Solid Fuel Stoves. *Fuel* **2010**, *89* (3), 782–791. https://doi.org/10.1016/j.fuel.2009.09.019.

(16) Falcitelli, M.; Pasini, S.; Rossi, N.; Tognotti, L. CFD+reactor Network Analysis: An Integrated Methodology for the Modeling and Optimisation of Industrial Systems for Energy Saving and Pollution Reduction. *Appl. Therm. Eng.* **2002**, *22* (8), 971–979. https://doi.org/10.1016/S1359-4311(02)00014-5.

(17) Weber, K.; Li, T.; Løvås, T.; Perlman, C.; Seidel, L.; Mauss, F. Stochastic Reactor Modeling of Biomass Pyrolysis and Gasification. *J. Anal. Appl. Pyrolysis* **2017**, *124*, 592–601. https://doi.org/10.1016/j.jaap.2017.01.003.

(18) Menage, D.; Lemaire, R.; Seers, P. Experimental Study and Chemical Reactor Network Modeling of the High Heating Rate Devolatilization and Oxidation of Pulverized Bituminous Coals under Air, Oxygen-Enriched Combustion (OEC) and Oxy-Fuel Combustion (OFC). *Fuel Process. Technol.* **2018**, *177* (April), 179–193. https://doi.org/10.1016/j.fuproc.2018.04.025.

(19) Stark, A. K.; Bates, R. B.; Zhao, Z.; Ghoniem, A. F. Prediction and Validation of Major Gas and Tar Species from a Reactor Network Model of Air-Blown Fluidized Bed Biomass Gasification. *Energy and Fuels* **2015**, *29* (4), 2437–2452. https://doi.org/10.1021/ef5027955.

(20) Ranzi, E.; Pierucci, S.; Aliprandi, P. C.; Stringa, S. Comprehensive and Detailed Kinetic Model of a Traveling Grate Combustor of Biomass. *Energy and Fuels* **2011**, *25* (9), 4195–4205. https://doi.org/10.1021/ef200902v.

(21) Jean-Pierre Leclerc, Roda Bounaceur, Olivier Herbinet, Frédérique Battin Leclerc,

Céline Le Dreff, et al., Modelization of the aeraulic in a wood-burning appliance. Tracer8, 8th international Conference on Tracers and Tracing Methods, Feb **2019**, 1, Đà Nẵng, Vietnam. ffhal-02390721.

(22) Das, B.; Bhattacharaya A.; Datta A. Kinetic modeling of biomass gasification and tar formation in a fluidized bed gasifier using equivalent reactor network (ERN). *Fuel* **2020**, *280* (November 2020), 0016-2361. https://doi.org/10.1016/j.fuel.2020.118582

(23) Dhahak, A.; Bounaceur, R.; Le Dreff-lorimier, C.; Schmidt, G.; Trouve, G.; Battin-Leclerc, F. Development of a Detailed Kinetic Model for the Combustion of Biomass. *Fuel* **2019**, *242* (October 2018), 756–774. https://doi.org/10.1016/j.fuel.2019.01.093.

(24) Ranzi E, Cuoci A, Faravelli T, Frassoldati A, Migliavacca G, Pierucci S, et al., Chemical kinetics of biomass pyrolysis. Energy Fuels 2008;22:4292–300.

(25) NF EN 13229, Foyers ouverts et inserts à combustibles solides – Exigences et méthodes d'essai, AFNOR – CEN, juin **2002**, 1-3.

(26) Stark, A. K.; Altantzis, C.; Bates, R. B.; Ghoniem, A. F. Towards an Advanced Reactor Network Modeling Framework for Fluidized Bed Biomass Gasification: Incorporating Information from Detailed CFD Simulations. *Chem. Eng. J.* **2016**, *303*, 409–424. https://doi.org/10.1016/j.cej.2016.06.026.

(27) Gogoi, B.; Baruah, D. C. Steady State Heat Transfer Modeling of Solid Fuel Biomass Stove: Part 1. *Energy* **2016**, *97*, 283–295. https://doi.org/10.1016/j.energy.2015.12.130.

(28) Arora, P.; Hoadley, A. F. A.; Mahajani, S. M.; Ganesh, A. Compartment Model for a Dual Fluidized Bed Biomass Gasifier. *Chem. Eng. Res. Des.* **2017**, *117*, 274–286. https://doi.org/10.1016/j.cherd.2016.10.025.

(29) Fichet, V.; Kanniche, M.; Plion, P.; Gicquel, O. A Reactor Network Model for Predicting NOx Emissions in an Industrial Natural Gas Burner. *Fuel* **2010**, *89*, 2202–2210. https://doi.org/10.1007/s40430-013-0039-5.

(30) Canada, R. naturelles. *Le Guide Au Chauffage Au Bois Résidentiel*; CMHC-SCHL; **2002**, 11-21. https://www.yumpu.com/fr/document/read/12332298/le-guide-du-chauffage-au-bois-residentiel-schl

(31) MATLAB, Matlab Statistics and Machine Learning Toolbox Release 2016a, The MathWorks Inc., **2016**, Natick, Massachusetts, United States.

(32) Debiagi, P. E. A.; Gentile, G.; Pelucchi, M.; Frassoldati, A.; Cuoci, A.; Faravelli, T.; Ranzi, E. Detailed Kinetic Mechanism of Gas-Phase Reactions of Volatiles Released from Biomass Pyrolysis. *Biomass and Bioenergy* **2016**, *93*, 60–71. https://doi.org/10.1016/j.biombioe.2016.06.015.

(33) Ranzi, E.; Debiagi, P.E.A.; Frassoldati, A. Mathematical Modeling of Fast Biomass Pyrolysis and Bio-oil Formation. **2017**, *ACS Sustainable Chemistry and Engineering* 5(4), pp. 2867-2881

(34) Fukutome A, Kawamoto H, Saka S. Processes forming gas tar, and coke in cellulose gasification from gas-phase reactions of levoglucosan as intermediate. *ChemSusChem* **2015**;8:2240–9.

(35) EJ, Nimlos MR, Evans RJ. Kinetic analysis of the gas-phase pyrolysis of carbohydrates. *Fuel* **2001**;80:1697–709

(36) Jenkins, B. .; Baxter, L. .; Miles, T. .; Miles, T. . Combustion Properties of Biomass. *Fuel Process. Technol.* **1998**, *54* (1-3), 17–46. https://doi.org/10.1016/S0378-3820(97)00059-3.

(37) Thornock, J.; Tree, D.; Xue, Y.; Sadasivuni, V.; Tsiava, R. Impact of Selective Oxygen Injection on NO, LOI, and Flame Luminosity in a Fine Particle, Swirl-Stabilized Wood Flame. In *8th US National Combustion Meeting 2013*; **2013**; Vol. 4.

(38) Panahi, A.; Levendis, Y. A.; Vorobiev, N.; Schiemann, M. Direct Observations on the Combustion Characteristics of Miscanthus and Beechwood Biomass Including Fusion and Spherodization. *Fuel Process. Technol.* **2017**, *166*, 41–49. https://doi.org/10.1016/j.fuproc.2017.05.029.

(39) Liu, C.; Yan, B.; Chen, G.; Bai, X. S. Structures and Burning Velocity of Biomass Derived Gas Flames. *Int. J. Hydrogen Energy* **2010**, *35* (2), 542–555. https://doi.org/10.1016/j.ijhydene.2009.11.020.

(40) Y. Song; L. Marrodán; N. Vin; O. Herbinet; E. Assaf; C. Fittschen; A. Stagni; T. Faravelli; M.U. Alzueta; F. Battin-Leclerc; The sensitizing effects of NO_2 and NO on methane low temperature oxidation in a jet stirred reactor, Proceedings of the Combustion Institute 37 (2019) 667–675. https://doi.org/10.1016/j.proci.2018.06.115

(41) Appel J. , Bockhorn, H., Frenklach, M.; Kinetic Modeling of Soot Formation with Detailed Chemistry and Physics: Laminar Premixed Flames of C 2 Hydrocarbons. *Combustion and flame* **2000**, 122-136; https://doi.org/10.1016/S0010-2180(99)00135-2.

(42) Victor Chernov, Murray J. Thomson, Seth B. Dworkin, Nadezhda A. Slavinskaya, Uwe Riedel; Soot formation with C1 and C2 fuels using an improved chemical mechanism for PAH growth; *Combustion and Flame* **2014**, 592-601, https://doi.org/10.1016/j.combustflame.2013.09.017.